

Analytic decay width of the Higgs boson to massive bottom quarks at order α_s^3

Jian Wang,^{b,c} Xing Wang,^{d,e} Yefan Wang^a

^a*Department of Physics and Institute of Theoretical Physics, Nanjing Normal University, Nanjing, Jiangsu 210023, China*

^b*School of Physics, Shandong University, Jinan, Shandong 250100, China*

^c*Center for High Energy Physics, Peking University, Beijing 100871, China*

^d*School of Science and Engineering, The Chinese University of Hong Kong, Shenzhen, Guangdong, 518172, China*

^e*Physik Department, TUM School of Natural Sciences, Technische Universität München, D - 85748 Garching, Germany*

E-mail: j.wang@sdu.edu.cn, xing.wang@tum.de, wangyefan@nnu.edu.cn

ABSTRACT: The Higgs boson decay into bottom quarks is the dominant decay channel contributing to its total decay width, which can be used to measure the bottom quark Yukawa coupling and mass. This decay width has been computed up to $\mathcal{O}(\alpha_s^4)$ for the process induced by the bottom quark Yukawa coupling, assuming massless final states, and the corresponding corrections beyond $\mathcal{O}(\alpha_s^2)$ are found to be less than 0.2%. We present an analytical result for the decay into massive bottom quarks at $\mathcal{O}(\alpha_s^3)$ that includes the contribution from the top quark Yukawa coupling induced process. We have made use of the optical theorem, canonical differential equations and the regular basis in the calculation and expressed the result in terms of multiple polylogarithms and elliptic functions. We propose a systematic and unified procedure to derive the ϵ -factorized differential equation for the three-loop kite integral family, which includes the three-loop banana integrals as a sub-sector. We find that the $\mathcal{O}(\alpha_s^3)$ corrections increase the decay width, relative to the result up to $\mathcal{O}(\alpha_s^2)$, by 1% due to the large logarithms $\log^i(m_H^2/m_b^2)$ with $1 \leq i \leq 4$ in the small bottom quark mass limit. The coefficient of the double logarithm is proportional to $C_A - C_F$, which is the typical color structure in the resummation of soft quark contributions at subleading power.

Contents

1	Introduction	1
2	Calculation framework	3
3	Calculation of master integrals	5
3.1	Canonical basis of the NP1 family	6
3.2	Boundary conditions	8
4	Renormalization	9
5	Analytic results	10
6	Asymptotic expansion	15
6.1	Small m_b limit of $\Gamma_{H \rightarrow b\bar{b}}$	15
6.2	Threshold limit	19
7	Numerical result	21
8	Conclusion	22
A	Topologies of the master integrals	24
B	The canonical form of the three-loop kite integral family	25
B.1	Banana sector	27
B.2	Higher sectors	28
B.3	Mixing	32
B.4	ϵ -factorized form	32

1 Introduction

After the discovery of the Higgs boson, precise measurements of its couplings are of great importance. The couplings with massive gauge bosons have been measured with an accuracy of 5%, and the Yukawa couplings of the Higgs boson to the top quark, bottom quark, and tau lepton have uncertainties of around 10% [1]. Among these couplings, the bottom Yukawa coupling y_b stands out for its dominant contribution to the Higgs boson total decay width. The expected uncertainty on the branching ratio measurements of $H \rightarrow b\bar{b}$ can reach 5% at the HL-LHC [2]. The signal strength of $H \rightarrow b\bar{b}$ at the CEPC can be measured with a statistical uncertainty of 0.27% after accumulating an integrated luminosity of 5.6 ab^{-1} [3, 4].

These promising experiments call for precise theoretical predictions. The next-to-leading order (NLO) QCD and electroweak (EW) corrections to the Higgs boson decay into massive bottom quarks have been computed long ago [5–10]. The NNLO QCD corrections were obtained numerically and analytically in refs. [11–13] and refs. [14–17], respectively. When the final-state bottom quark is taken to be massless, the total and differential decay rates are known up to $\mathcal{O}(y_b^2\alpha_s^4)$ [18–21] and $\mathcal{O}(y_b^2\alpha_s^3)$ [22–25], respectively¹. It is found that the higher-order corrections beyond NNLO are less than 0.2%. The mixed QCD×EW corrections have been considered in [27, 28] and turn out to decrease the decay width by about 1%. The matching to parton shower [29, 30] and the higher-order corrections to the $H \rightarrow bbj$ [31] and $H \rightarrow b\bar{b}b\bar{b}$ [32] processes have also been investigated. The process induced by the top quark Yukawa coupling y_t could contribute to the decay width of $H \rightarrow b\bar{b}$ at two-loop level [17], and even higher-order corrections have been obtained numerically when the top quark loop is integrated out in the large mass limit [33]².

In this paper we are going to provide an analytic form of the $H \rightarrow b\bar{b}$ decay width at QCD N³LO by including the finite bottom quark mass effect in the contribution induced by the top quark Yukawa coupling y_t . This is an extension of our previous work [14], in which we present a full analytic result of the QCD NNLO correction to the $H \rightarrow b\bar{b}$ decay induced by the bottom quark Yukawa coupling y_b . We find that the finite bottom quark mass effect at $\mathcal{O}(\alpha_s^2)$ is below one percent compared to the result with massless final-state bottom quarks at $\mathcal{O}(\alpha_s^2)$, since the corresponding decay rate can be Taylor expanded in $m_b^2/m_H^2 \sim 5 \times 10^{-4}$. Therefore we neglect the bottom quark mass in the $\mathcal{O}(\alpha_s^3)$ corrections to the y_b induced processes. By contrast, the contribution from the y_t coupling is enhanced by logarithmic terms $\log^i(m_H^2/m_b^2)$ from $\mathcal{O}(\alpha_s^2)$ and even power-enhanced from $\mathcal{O}(\alpha_s^3)$. The former has aroused interest in the subleading power resummation recently and makes more significant contributions to the decay width than naive expectation with perturbative expansion in α_s . The latter indicates that the contribution is not proportional to the bottom Yukawa coupling at leading power. These new features can only be unveiled by an analytical calculation. Moreover, we have obtained analytical results in different schemes of the mass renormalization so that we are able to estimate the uncertainties associating with the renormalization schemes.

The rest of this paper is organized as follows. In section 2, we introduce the calculation framework including the effective operators. The requisite master integrals are calculated analytically in section 3. After a brief description of the renormalization in section 4, we present the full analytic result in section 5. The asymptotic expansion is discussed in section 6 and the numerical results are investigated in section 7. We conclude in section 8. The topological diagrams of the master integrals are shown in appendix A. We describe a systematic and unified procedure to derive an ϵ -factorized differential equation for the three-loop kite integral family that contains three-loop banana integrals as a sub-sector in appendix B.

¹The kinematical π^2 terms are resummed in ref. [26].

²Such corrections to the Higgs decay into all hadronic states, including both bottom quarks and gluons, are available up to $\mathcal{O}(\alpha_s^4)$ [34, 35] when the bottom quark mass is neglected except for that in the couplings.

2 Calculation framework

At the leading order (LO), the decay of a Higgs boson to a massive bottom quark pair is induced by the bottom Yukawa coupling. However, the top quark Yukawa coupling starts to contribute to the decay at higher orders in α_s . The top quark loop can be integrated in the large top quark mass limit, leading to an effective coupling between the Higgs boson and the gluons. This approximation works exceedingly well with a relative error at the percent level [17]. As such, the effective Lagrangian [35–38] that is relevant to Higgs boson decay to massive bottom quarks can be written as

$$\mathcal{L}_{\text{eff}} = -\frac{H}{v} (C_1 \mathcal{O}_1^R + C_2 \mathcal{O}_2^R) + \mathcal{L}_{\text{QCD}}, \quad (2.1)$$

where v is the vacuum expectation value of the Higgs field, \mathcal{L}_{QCD} is the QCD Lagrangian without top quarks and only bottom quarks are considered massive. The two renormalized operators are defined by

$$\mathcal{O}_1^R = Z_{11} \mathcal{O}_1 + Z_{12} \mathcal{O}_2, \quad \mathcal{O}_2^R = Z_{21} \mathcal{O}_1 + Z_{22} \mathcal{O}_2 \quad (2.2)$$

with

$$\mathcal{O}_1 = (G_{a,\mu\nu}^0)^2, \quad \mathcal{O}_2 = m_b^0 \bar{b}^0 b^0. \quad (2.3)$$

The superscript “0” indicates the bare quantity. The renormalization constant $Z_{21} = 0$ in the $\overline{\text{MS}}$ scheme due to the Ward identity in the process $H \rightarrow gg$ via a bottom loop, and $Z_{22} = 1$ because of our choice of the bare quantities in \mathcal{O}_2 . The renormalization constants Z_{11} and Z_{12} [38] can be derived from Z_{α_s} and Z_m in the $\overline{\text{MS}}$ scheme,

$$\begin{aligned} Z_{11} &= 1 + \alpha_s \frac{\partial \log Z_{\alpha_s}}{\partial \alpha_s} = 1 + \left(\frac{\alpha_s}{\pi}\right) \left(\frac{-11C_A + 2n_f}{12\epsilon}\right) \\ &\quad + \left(\frac{\alpha_s}{\pi}\right)^2 \left(\frac{(-11C_A + 2n_f)^2}{144\epsilon^2} - \frac{17C_A^2 - 5C_A n_f - 3C_F n_f}{24\epsilon}\right) + \mathcal{O}(\alpha_s^3), \\ Z_{12} &= -4\alpha_s \frac{\partial \log Z_m^{\overline{\text{MS}}}}{\partial \alpha_s} = \left(\frac{\alpha_s}{\pi}\right) \left(\frac{3C_F}{\epsilon}\right) \\ &\quad + \left(\frac{\alpha_s}{\pi}\right)^2 C_F \left(\frac{-11C_A + 2n_f}{4\epsilon^2} + \frac{97C_A + 9C_F - 10n_f}{24\epsilon}\right) + \mathcal{O}(\alpha_s^3). \end{aligned} \quad (2.4)$$

where C_A and C_F are the QCD color factors and n_f denotes the number of active quark flavors. The Wilson coefficients of the effective operators are given by [35, 38–40]

$$\begin{aligned} C_1 &= -\left(\frac{\alpha_s}{\pi}\right) \frac{1}{12} - \left(\frac{\alpha_s}{\pi}\right)^2 \frac{11}{48} \\ &\quad - \left(\frac{\alpha_s}{\pi}\right)^3 \left[\frac{2777}{3456} + \frac{19}{192} L_t - n_f \left(\frac{67}{1152} - \frac{1}{36} L_t \right) \right] + \mathcal{O}(\alpha_s^4), \\ C_2 &= 1 + \left(\frac{\alpha_s}{\pi}\right)^2 \left[\frac{5}{18} - \frac{1}{3} L_t \right] \\ &\quad + \left(\frac{\alpha_s}{\pi}\right)^3 \left[-\frac{841}{1296} + \frac{5}{3} \zeta(3) - \frac{79}{36} L_t - \frac{11}{12} L_t^2 + n_f \left(\frac{53}{216} + \frac{1}{18} L_t^2 \right) \right] + \mathcal{O}(\alpha_s^4), \end{aligned} \quad (2.5)$$

where $L_t = \log(\mu^2/m_t^2)$ and m_t is the top quark mass in the on-shell scheme. In the above expressions, the color factors $C_F = 4/3$, $C_A = 3$, $T_R = 1/2$ have been substituted. Note that C_1 starts from $\mathcal{O}(\alpha_s)$ and that the first nontrivial QCD corrections in C_2 begin at $\mathcal{O}(\alpha_s^2)$.

According to the combination structure of effective operators in the squared amplitudes, the decay width of $H \rightarrow b\bar{b}$ can be decomposed into three parts, i.e.,

$$\Gamma_{H \rightarrow b\bar{b}} = \Gamma_{H \rightarrow b\bar{b}}^{C_2 C_2} + \Gamma_{H \rightarrow b\bar{b}}^{C_1 C_2} + \Gamma_{H \rightarrow b\bar{b}}^{C_1 C_1}. \quad (2.6)$$

Each of them can be expanded in a series of the strong coupling α_s ,

$$\begin{aligned} \Gamma_{H \rightarrow b\bar{b}}^{C_2 C_2} &= C_2 C_2 \left[\Delta_{0,b\bar{b}}^{C_2 C_2} + \left(\frac{\alpha_s}{\pi}\right) \Delta_{1,b\bar{b}}^{C_2 C_2} + \left(\frac{\alpha_s}{\pi}\right)^2 \Delta_{2,b\bar{b}}^{C_2 C_2} + \left(\frac{\alpha_s}{\pi}\right)^3 \Delta_{3,b\bar{b}}^{C_2 C_2} + \mathcal{O}(\alpha_s^4) \right], \\ \Gamma_{H \rightarrow b\bar{b}}^{C_1 C_2} &= C_1 C_2 \left[\left(\frac{\alpha_s}{\pi}\right) \Delta_{1,b\bar{b}}^{C_1 C_2} + \left(\frac{\alpha_s}{\pi}\right)^2 \Delta_{2,b\bar{b}}^{C_1 C_2} + \mathcal{O}(\alpha_s^3) \right], \\ \Gamma_{H \rightarrow b\bar{b}}^{C_1 C_1} &= C_1 C_1 \left[\left(\frac{\alpha_s}{\pi}\right) \Delta_{1,b\bar{b}}^{C_1 C_1} + \mathcal{O}(\alpha_s^2) \right], \end{aligned} \quad (2.7)$$

where we have written down explicitly the terms that are needed to obtain $\Gamma_{H \rightarrow b\bar{b}}$ to $\mathcal{O}(\alpha_s^3)$. Note that the leading orders of $\Gamma_{H \rightarrow b\bar{b}}^{C_1 C_2}$ and $\Gamma_{H \rightarrow b\bar{b}}^{C_1 C_1}$ are $\mathcal{O}(\alpha_s^2)$ and $\mathcal{O}(\alpha_s^3)$, respectively.

The analytic results of $\Delta_{i,b\bar{b}}^{C_2 C_2}$ have been calculated up to $\mathcal{O}(\alpha_s^4)$ and $\mathcal{O}(\alpha_s^2)$ in the massless³ [19–21] and massive [14] bottom quark cases, respectively. It is found that the massless result can be obtained from the massive one by taking the limit continuously. Therefore, it is reasonable to take $\Delta_{3,b\bar{b}}^{C_2 C_2}$ calculated in [19, 21] as the result for the decay into massive bottom quarks, since the relative error is expected to be below one percent.

In this paper, we present analytic results of $\Delta_{1,b\bar{b}}^{C_1 C_1}$, $\Delta_{1,b\bar{b}}^{C_1 C_2}$ and $\Delta_{2,b\bar{b}}^{C_1 C_2}$ with full dependence on the bottom quark mass. These results cannot be Taylor expanded in m_b^2 because of the logarithmic dependence. These large logarithms make a significant contribution to the corrections and may sabotage a perturbative expansion in α_s . They are different from the traditional large logarithms induced by soft gluons, and their all-order structure is an interesting topic under active research.

We compute the decay width of $H \rightarrow b\bar{b}$ via the optical theorem, i.e.,

$$\Gamma_{H \rightarrow b\bar{b}} = \frac{\text{Im}_{b\bar{b}}(\Sigma)}{m_H}, \quad (2.8)$$

where Σ represents the amplitude of the process $H \rightarrow b\bar{b} \rightarrow H$ and the imaginary part is obtained by taking the cut on at least one bottom quark pair. Specifically, $\Delta_{1,b\bar{b}}^{C_1 C_1}$ and $\Delta_{1,b\bar{b}}^{C_1 C_2}$ require the calculation of two-loop Feynman diagrams; see, e.g., figure 1 (a) and (b). $\Delta_{2,b\bar{b}}^{C_1 C_2}$ is obtained after calculating the three-loop Feynman diagrams, such as figure 1 (c)-(f). Note that the imaginary part receives a contribution also from the cut on the four bottom quarks, e.g., in figure 1 (c). For clarity, we define

$$\Delta_{2,b\bar{b}}^{C_1 C_2} \equiv \tilde{\Delta}_{2,b\bar{b}}^{C_1 C_2} + \Delta_{2,b\bar{b}\bar{b}\bar{b}}^{C_1 C_2} \quad (2.9)$$

where $\tilde{\Delta}_{2,b\bar{b}}^{C_1 C_2}$ represents the correction from the final states of $b\bar{b}$, $b\bar{b}g$, $b\bar{b}gg$, and $b\bar{b}q\bar{q}$, while $\Delta_{2,b\bar{b}\bar{b}\bar{b}}^{C_1 C_2}$ gets contribution from the final state of $b\bar{b}\bar{b}\bar{b}$.

³The bottom quark Yukawa coupling is still finite.

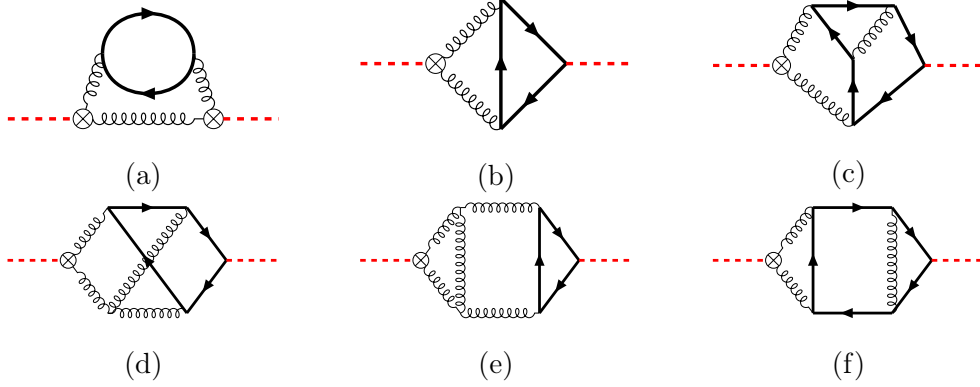


Figure 1: Sample Feynman diagrams contributing to $\Delta_{1,b\bar{b}}^{C_1C_1}$, $\Delta_{1,b\bar{b}}^{C_1C_2}$ and $\Delta_{2,b\bar{b}}^{C_1C_2}$. (a) and (b) are the two-loop diagrams of $\Delta_{1,b\bar{b}}^{C_1C_1}$ and $\Delta_{1,b\bar{b}}^{C_1C_2}$, respectively. (c)-(f) are typical three-loop diagrams of $\Delta_{2,b\bar{b}}^{C_1C_2}$. The crossed dots stand for the effective Hgg vertices. The thick black and red lines denote the massive bottom quark and the Higgs boson, respectively.

Below we focus on the three-loop calculations of $\Delta_{2,b\bar{b}}^{C_1C_2}$, as the two-loop Feynman diagrams are easier to compute. We have generated the Feynman diagrams and corresponding amplitudes of $H \rightarrow b\bar{b} \rightarrow H$ with effective vertices using the package `FeynArts` [41]. The model including the effective operators is implemented via `FeynRules` [42]. Then the package `FeynCalc` [43, 44] is used to simplify the Dirac matrices. The amplitudes are expressed as linear combinations of scalar integrals, which can be reduced to a set of basis integrals called master integrals (MIs) due to the identities from integration by parts (IBP) [45, 46]. In this procedure, we used the package `Kira` [47] to perform the reduction. Some MIs can be factorized into one- and two-loop integrals and are easy to compute. After considering the symmetries among integrals with the help of the package `CalcLoop`⁴, the other MIs can be classified into two integral families (denoted as NP1 and P1), as shown in figure 2.

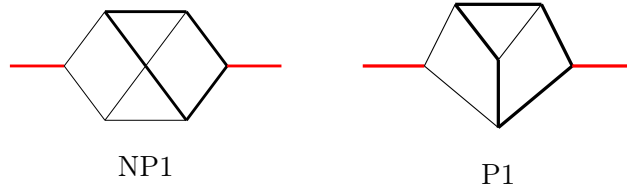


Figure 2: The topologies of the NP1 and P1 integral families. The thick black and red lines stand for the massive bottom quark and the Higgs boson, respectively. The other lines represent massless particles.

3 Calculation of master integrals

As mentioned in eq. (2.9), we need to calculate the MIs with two and four bottom quark final states separately. In the latter case, we find 10 MIs, some of which are depicted in

⁴<https://gitlab.com/multiloop-pku/calclloop>

figure 3. One can choose the regular basis in which all MIs start from $\mathcal{O}(\epsilon^0)$ and the higher order terms in ϵ are not required in the amplitude [48]. The analytical results of the first 9 basis integrals can be found in [48]. They are expressed either as complete elliptic integrals of the first kind or one-fold integrals of them. The last MI corresponding to figure 3(c) appears in the basis of the integral family but does not contribute to $\Delta_{2,b\bar{b}\bar{b}\bar{b}}^{C_1 C_2}$. However, given that this integral is interesting for the calculation of general elliptic integral families, we describe the procedure to construct the ϵ -factorized form of the differential equation in appendix B.

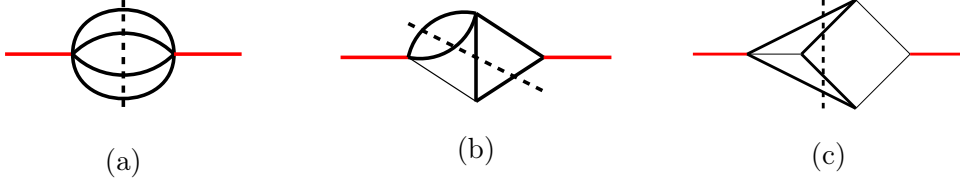


Figure 3: Typical MIs in calculation of $\Delta_{2,b\bar{b}\bar{b}\bar{b}}^{C_1 C_2}$. The cutting line passes through four bottom quarks. The thick black and red lines stand for the massive bottom quark and the Higgs boson, respectively. The other lines represent massless particles.

Then we turn to the calculations of MIs contributing to $\tilde{\Delta}_{2,b\bar{b}}^{C_1 C_2}$. The topology diagrams of the MIs in the NP1 and P1 families are displayed in figure 6 and figure 7, respectively, in appendix A. We adopt the method of differential equations [49, 50]. After choosing the proper basis, the differential equation exhibits a canonical form, i.e., the dimension parameter ϵ is factorized from the kinematic dependence. Then the differential equations can be solved recursively in terms of multiple polylogarithms (MPLs) [51], which are defined by $G(x) \equiv 1$ and

$$G(l_1, l_2, \dots, l_n, x) \equiv \int_0^x \frac{dt}{t - l_1} G(l_2, \dots, l_n, t), \quad (3.1)$$

$$G(\vec{0}_n, x) \equiv \frac{1}{n!} \ln^n x. \quad (3.2)$$

The number of elements in the set $\{l_1, l_2, \dots, l_n\}$ is referred to as the transcendental *weight* of the MPLs. Below we only show the canonical basis of the NP1 family because the MIs in the P1 family can be either found in the NP1 family or our previous papers [14, 52].

3.1 Canonical basis of the NP1 family

The integrals in the NP1 family are represented by

$$I_{n_1, n_2, \dots, n_9}^{\text{NP1}} = \text{Im}_{b\bar{b}} \int \prod_{i=1}^3 \frac{(m_b^2)^\epsilon d^D q_i}{i\pi^{D/2} \Gamma(1 + \epsilon)} \frac{D_8^{-n_8} D_9^{-n_9}}{D_1^{n_1} D_2^{n_2} D_3^{n_3} D_4^{n_4} D_5^{n_5} D_6^{n_6} D_7^{n_7}}, \quad (3.3)$$

with $D = 4 - 2\epsilon$ and all $n_i \geq 0, i = 1, \dots, 8, n_9 \leq 0$. The denominators D_i read

$$\begin{aligned} D_1 &= q_1^2, & D_2 &= (q_1 - q_2)^2 - m_b^2, & D_3 &= q_2^2 - m_b^2, \\ D_4 &= q_3^2 - m_b^2, & D_5 &= (q_2 + q_3)^2, & D_6 &= (q_3 - k)^2 - m_b^2, \end{aligned}$$

$$D_7 = (q_1 + k)^2, \quad D_8 = (q_1 - q_2 - q_3 + k)^2, \quad D_9 = (q_2 - k)^2, \quad (3.4)$$

where the Feynman prescription $+i\epsilon$ has been suppressed. The external momentum k satisfies $k^2 = m_H^2$. In the above definition of integrals, we have required only the imaginary contribution induced by a cut on a bottom quark pair.

There are 30 master integrals contributing to $\tilde{\Delta}_{2,bb}^{C_1 C_2}$. To construct the canonical basis, we first select

$$\begin{aligned}
M_1^{\text{NP1}} &= \epsilon^3 m_b^2 I_{0,2,2,2,0,1,0,0,0}^{\text{NP1}}, & M_2^{\text{NP1}} &= \epsilon^3 m_b^2 I_{0,2,2,0,1,2,0,0,0}^{\text{NP1}}, \\
M_3^{\text{NP1}} &= \epsilon^3 m_b^2 I_{0,2,2,0,2,1,0,0,0}^{\text{NP1}}, & M_4^{\text{NP1}} &= \epsilon^3 m_b^2 I_{2,2,0,0,1,2,0,0,0}^{\text{NP1}}, \\
M_5^{\text{NP1}} &= \epsilon^3 m_b^2 I_{2,2,0,0,2,1,0,0,0}^{\text{NP1}}, & M_6^{\text{NP1}} &= (1-2\epsilon)\epsilon m_b^4 I_{1,3,0,0,1,3,0,0,0}^{\text{NP1}}, \\
M_7^{\text{NP1}} &= \epsilon^3 m_b^4 I_{2,2,0,2,0,1,1,0,0}^{\text{NP1}}, & M_8^{\text{NP1}} &= \epsilon^3 m_b^4 I_{2,0,2,0,1,2,1,0,0}^{\text{NP1}}, \\
M_9^{\text{NP1}} &= \epsilon^3 m_b^4 I_{2,0,2,0,2,1,1,0,0}^{\text{NP1}}, & M_{10}^{\text{NP1}} &= \epsilon^3 m_b^4 I_{0,2,2,2,0,1,1,0,0}^{\text{NP1}}, \\
M_{11}^{\text{NP1}} &= \epsilon^3 m_b^4 I_{0,2,1,2,0,1,2,0,0}^{\text{NP1}}, & M_{12}^{\text{NP1}} &= (1-2\epsilon)\epsilon^3 m_b^2 I_{2,2,0,1,1,1,0,0,0}^{\text{NP1}}, \\
M_{13}^{\text{NP1}} &= \epsilon^3 m_b^2 I_{0,2,1,0,1,2,1,0,0}^{\text{NP1}}, & M_{14}^{\text{NP1}} &= \epsilon^2 m_b^4 I_{0,3,1,0,1,2,1,0,0}^{\text{NP1}}, \\
M_{15}^{\text{NP1}} &= (1-2\epsilon)\epsilon^4 m_b^2 I_{0,1,2,0,1,1,1,1,0}^{\text{NP1}}, & M_{16}^{\text{NP1}} &= (1-2\epsilon)\epsilon^3 m_b^2 I_{1,2,0,1,1,0,0,2,0}^{\text{NP1}}, \\
M_{17}^{\text{NP1}} &= (1-2\epsilon)\epsilon^4 m_b^2 I_{1,2,0,1,1,0,1,1,0}^{\text{NP1}}, & M_{18}^{\text{NP1}} &= \epsilon^3 m_b^4 I_{2,0,0,2,2,1,0,1,0}^{\text{NP1}}, \\
M_{19}^{\text{NP1}} &= (1-2\epsilon)\epsilon^4 m_b^2 I_{1,2,0,1,1,1,1,0,0}^{\text{NP1}}, & M_{20}^{\text{NP1}} &= (1-2\epsilon)\epsilon^3 m_b^4 I_{1,2,0,2,1,1,1,0,0}^{\text{NP1}}, \\
M_{21}^{\text{NP1}} &= (1-2\epsilon)\epsilon^3 m_b^4 I_{1,3,0,1,1,1,1,0,0}^{\text{NP1}}, & M_{22}^{\text{NP1}} &= (1-2\epsilon)\epsilon^4 m_b^2 I_{1,1,1,0,1,2,1,0,0}^{\text{NP1}}, \\
M_{23}^{\text{NP1}} &= (1-2\epsilon)\epsilon^4 m_b^2 I_{0,2,1,1,1,1,1,0,0}^{\text{NP1}}, & M_{24}^{\text{NP1}} &= (1-2\epsilon)\epsilon^4 m_b^2 I_{1,1,1,1,1,0,0,2,0}^{\text{NP1}}, \\
M_{25}^{\text{NP1}} &= (1-2\epsilon)\epsilon^4 m_b^2 I_{2,1,0,1,1,1,0,1,0}^{\text{NP1}}, & M_{26}^{\text{NP1}} &= (1-2\epsilon)\epsilon^5 m_b^2 I_{1,1,1,1,1,1,1,0,0}^{\text{NP1}}, \\
M_{27}^{\text{NP1}} &= (1-2\epsilon)\epsilon^4 m_b^4 I_{1,1,1,2,1,1,1,0,0}^{\text{NP1}}, & M_{28}^{\text{NP1}} &= (1-2\epsilon)\epsilon^5 m_b^2 I_{1,1,1,1,1,1,1,0,1,0}^{\text{NP1}}, \\
M_{29}^{\text{NP1}} &= (1-2\epsilon)\epsilon^4 m_b^4 I_{1,1,1,2,1,1,0,1,0}^{\text{NP1}}, & M_{30}^{\text{NP1}} &= (1-2\epsilon)\epsilon^5 m_b^4 I_{1,1,1,1,1,1,1,1,0}^{\text{NP1}}. \quad (3.5)
\end{aligned}$$

Here all M_i^{NP1} are dimensionless. We define the dimensionless variable $z \equiv m_H^2/m_b^2$. Then we obtain the following canonical basis of the NP1 family:

$$\begin{aligned}
F_1^{\text{NP1}} &= M_1^{\text{NP1}} r, & F_2^{\text{NP1}} &= M_2^{\text{NP1}}(-z), & F_3^{\text{NP1}} &= \frac{M_2^{\text{NP1}} r}{2} + M_3^{\text{NP1}} r, \\
F_4^{\text{NP1}} &= M_4^{\text{NP1}}(-z), & F_5^{\text{NP1}} &= (M_4^{\text{NP1}} + M_5^{\text{NP1}})(-r), & F_6^{\text{NP1}} &= \frac{M_5^{\text{NP1}}(z-4)}{4} + M_6^{\text{NP1}}, \\
F_7^{\text{NP1}} &= M_7^{\text{NP1}} r(-z), & F_8^{\text{NP1}} &= M_8^{\text{NP1}} z^2, & F_9^{\text{NP1}} &= \frac{M_8^{\text{NP1}} r z}{2} + M_9^{\text{NP1}} r z, \\
F_{10}^{\text{NP1}} &= M_{10}^{\text{NP1}} r z, & F_{11}^{\text{NP1}} &= \frac{M_{10}^{\text{NP1}}(z-4)}{2} z + M_{11}^{\text{NP1}}(z-4)z, \\
F_{12}^{\text{NP1}} &= -\frac{M_4^{\text{NP1}} r(7z-12)}{12(4-z)} + \frac{M_{12}^{\text{NP1}} r}{4-z} - \frac{M_6^{\text{NP1}} r}{3(4-z)} + \frac{M_5^{\text{NP1}} r}{12}, \\
F_{13}^{\text{NP1}} &= M_2^{\text{NP1}} + M_4^{\text{NP1}} + M_{13}^{\text{NP1}}(1-z)(2\epsilon+1) + M_{14}^{\text{NP1}}(4-4z)\epsilon + M_{15}^{\text{NP1}} \left(1 - \frac{z}{4}\right), \\
F_{14}^{\text{NP1}} &= \frac{M_2^{\text{NP1}} r(z-8)}{8(z-4)} + \frac{M_4^{\text{NP1}} r(z-3)}{2(z-4)} + \frac{M_{13}^{\text{NP1}} r(2(z+1)\epsilon + z-3)}{2(z-4)} \\
&\quad + \frac{M_{14}^{\text{NP1}} r(2z\epsilon-1)}{z-4} + \frac{M_{15}^{\text{NP1}} r(z-3)}{2(z-4)}, & F_{15}^{\text{NP1}} &= M_{15}^{\text{NP1}}(-z),
\end{aligned}$$

$$\begin{aligned}
F_{16}^{\text{NP1}} &= \frac{M_4^{\text{NP1}}r}{3} - \frac{M_5^{\text{NP1}}r(z-4)}{6z} - \frac{2M_6^{\text{NP1}}r}{3z} - \frac{M_8^{\text{NP1}}rz}{2} + M_{16}^{\text{NP1}}r + M_{17}^{\text{NP1}}r, \\
F_{17}^{\text{NP1}} &= M_{17}^{\text{NP1}}(-z), \quad F_{18}^{\text{NP1}} = M_{18}^{\text{NP1}}(-r)z, \quad F_{19}^{\text{NP1}} = M_{19}^{\text{NP1}}(-z), \\
F_{20}^{\text{NP1}} &= \frac{M_4^{\text{NP1}}r}{3} - \frac{M_5^{\text{NP1}}r(z-4)}{6z} - \frac{2M_6^{\text{NP1}}r}{3z} + \frac{3M_{19}^{\text{NP1}}r}{2} + M_{20}^{\text{NP1}}r + M_{21}^{\text{NP1}}r, \\
F_{21}^{\text{NP1}} &= M_{21}^{\text{NP1}}(-z), \quad F_{22}^{\text{NP1}} = M_{22}^{\text{NP1}}(-z), \quad F_{23}^{\text{NP1}} = M_{23}^{\text{NP1}}(-z), \quad F_{24}^{\text{NP1}} = M_{24}^{\text{NP1}}(-z), \\
F_{25}^{\text{NP1}} &= M_{25}^{\text{NP1}}(-z), \quad F_{26}^{\text{NP1}} = M_{26}^{\text{NP1}}(-z), \\
F_{27}^{\text{NP1}} &= \frac{M_2^{\text{NP1}}(z+4)r}{4(z-2)} + \frac{M_4^{\text{NP1}}(2z+3)r}{3(z-2)} - \frac{M_5^{\text{NP1}}(z-4)r}{12(z-2)} + \frac{M_6^{\text{NP1}}r}{6-3z} + \frac{M_8^{\text{NP1}}rz^2}{8-4z} \\
&\quad + \frac{M_{13}^{\text{NP1}}(2\epsilon+1)(1-z)r}{z-2} + \frac{M_{15}^{\text{NP1}}(z+2)r}{2(z-2)} + \frac{4M_{14}^{\text{NP1}}\epsilon(1-z)r}{z-2} + \frac{M_{19}^{\text{NP1}}rz}{2(z-2)} \\
&\quad + \frac{M_{21}^{\text{NP1}}rz}{z-2} + \frac{M_{22}^{\text{NP1}}rz}{4-2z} + \frac{M_{26}^{\text{NP1}}rz}{2-z} + \frac{M_{27}^{\text{NP1}}rz}{2-z}, \quad F_{28}^{\text{NP1}} = M_{28}^{\text{NP1}}(-z), \\
F_{29}^{\text{NP1}} &= \frac{M_{24}^{\text{NP1}}r}{2} - \frac{M_{25}^{\text{NP1}}r}{2} + M_{28}^{\text{NP1}}r + M_{29}^{\text{NP1}}r, \quad F_{30}^{\text{NP1}} = M_{30}^{\text{NP1}}z^2,
\end{aligned} \tag{3.6}$$

where

$$r = \sqrt{z(z-4)}. \tag{3.7}$$

To rationalize the square root r , we write

$$z = -\frac{(w-1)^2}{w} \tag{3.8}$$

with $-1 < w < 0$. Then r is rationalized to

$$r = \frac{(w+1)(w-1)}{w}. \tag{3.9}$$

The differential equations for the canonical basis $\mathbf{F}^{\text{NP1}} = (F_1^{\text{NP1}}, \dots, F_{30}^{\text{NP1}})^T$ become

$$\frac{d\mathbf{F}^{\text{NP1}}}{dw} = \epsilon \left(\sum_{i=1}^5 \frac{\mathbf{N}_i^{\text{NP1}}}{w - l_i^{\text{NP1}}} \right) \mathbf{F}^{\text{NP1}} \tag{3.10}$$

with $\mathbf{N}_i^{\text{NP1}}$ being constant rational matrices and

$$l_1^{\text{NP1}} = 0, \quad l_2^{\text{NP1}} = 1, \quad l_3^{\text{NP1}} = -1, \quad l_4^{\text{NP1}} = \frac{1 + \sqrt{3}i}{2}, \quad l_5^{\text{NP1}} = \frac{1 - \sqrt{3}i}{2}. \tag{3.11}$$

3.2 Boundary conditions

After solving the canonical differential equations, the results are written as the linear combinations of MPLs [51] with undetermined integration constants, where the MPLs can be evaluated using the `PolyLogTools` package [53] based on `GiNac` [54]. In another method, we get the high-precision numerical results of the basis integrals using the package `AMFlow` [55–58]. Notice that we have set the specific cuts corresponding to a bottom quark pair, excluding the cuts on four bottom quarks or two gluons. Explicit examples with more details on this method can be found in [52]. Comparing the two results, we obtain the numerical results of the integration constants. The analytical form is reproduced using the PSLQ algorithm [59]. It turns out that the constants consist of $\zeta(n)$ and π^n .

4 Renormalization

The results of the cut three-loop diagrams contain ultra-violet divergences, which would cancel after considering the renormalization of the mass, couplings, and effective operators.

In our calculation, the Higgs boson and the bottom quark are taken to be massive while the other light quarks are massless. The bottom quark mass appears in the Yukawa coupling and the loop propagators. In the Yukawa coupling, the bottom quark mass is renormalized in the $\overline{\text{MS}}$ scheme as in [14], i.e., $m_b^0 = Z_{m_b}^{\overline{\text{MS}}} m_b$, in order to avoid large logarithms in $\Gamma_{b\bar{b}}^{C_2 C_2}$; see e.g., [11, 14] for more details. The bottom quark mass in the propagators is renormalized in the on-shell scheme by default, i.e., $m_b^0 = Z_m^{\text{OS}} m_b$, and a comparison of the results in the $\overline{\text{MS}}$ and on-shell schemes is given in section 7. The renormalization of the strong coupling α_s is performed in the $\overline{\text{MS}}$ scheme, i.e., $\alpha_s^0 C_\epsilon = \mu^{2\epsilon} \alpha_s Z_{\alpha_s}$ with $C_\epsilon = (4\pi e^{-\gamma_E})^\epsilon$. The needed renormalization constants are given by [60–63]

$$\begin{aligned}
Z_{\alpha_s} &= 1 + \left(\frac{\alpha_s}{4\pi}\right) \frac{2n_l - 31}{3\epsilon} + \left(\frac{\alpha_s}{4\pi}\right)^2 \left(\frac{(31 - 2n_l)^2}{9\epsilon^2} + \frac{19n_l - 134}{3\epsilon} \right), \\
Z_{m_b}^{\overline{\text{MS}}} &= 1 - \left(\frac{\alpha_s}{4\pi}\right) \frac{4}{\epsilon} + \left(\frac{\alpha_s}{4\pi}\right)^2 \left(\frac{2(43 - 2n_l)}{3\epsilon^2} + \frac{10n_l - 293}{9\epsilon} \right), \\
Z_{m_b}^{\text{OS}} &= 1 + \left(\frac{\alpha_s}{4\pi}\right) D_\epsilon \left(-\frac{4}{\epsilon} - \frac{16}{3} - \frac{32\epsilon}{3} - \frac{64\epsilon^2}{3} \right) \\
&\quad + \left(\frac{\alpha_s}{4\pi}\right)^2 D_\epsilon^2 \left(\frac{86 - 4n_l}{3\epsilon^2} + \frac{10n_l - 101}{9\epsilon} + \frac{4(2n_l - 31)}{3\epsilon} \log\left(\frac{\mu^2}{m_b^2}\right) \right. \\
&\quad + \frac{2(31 - 2n_l)}{3} \log^2\left(\frac{\mu^2}{m_b^2}\right) + \frac{16(2n_l - 31)}{9} \log\left(\frac{\mu^2}{m_b^2}\right) + \frac{(10n_l - 79)\pi^2}{9} \\
&\quad \left. + \frac{(142n_l - 2251)}{18} + \frac{8\zeta(3)}{3} - \frac{16\pi^2 \log(2)}{9} \right), \tag{4.1}
\end{aligned}$$

where $n_l = n_f - 1$ is the number of massless quarks and

$$D_\epsilon \equiv e^{\gamma_E \epsilon} \Gamma(1 + \epsilon) \left(\frac{\mu^2}{m_b^2} \right)^\epsilon. \tag{4.2}$$

Besides, the mixing between the two effective operators indicates

$$\langle b\bar{b} | \mathcal{O}_1^R | H \rangle = Z_{11} \langle b\bar{b} | \mathcal{O}_1 | H \rangle + Z_{12} \langle b\bar{b} | \mathcal{O}_2 | H \rangle. \tag{4.3}$$

Part of the ultra-violet divergences in the loop amplitude of $\langle b\bar{b} | \mathcal{O}_1 | H \rangle$ has to be canceled with $Z_{12} \langle b\bar{b} | \mathcal{O}_2 | H \rangle$. Because Z_{12} starts from $\mathcal{O}(\alpha_s)$, the amplitude of $\langle b\bar{b} | \mathcal{O}_2 | H \rangle$ is of lower loop order. The bottom quark mass in $\langle b\bar{b} | \mathcal{O}_1 | H \rangle$ appears only in the propagator, and thus the mass in \mathcal{O}_2 must also be renormalized in the on-shell scheme to ensure the cancellation of divergences. After cancellation of divergences, we are free to convert the mass from one renormalization scheme to another.

5 Analytic results

After renormalization, we obtain the finite analytic results. The result of $\Delta_{1,bb}^{C_1C_1}$ is

$$\begin{aligned} \Delta_{1,bb}^{C_1C_1} &= \frac{m_H^3}{12v^2\pi} C_A C_F \left[\frac{2(w+1)^2 (w^4 - 8w^3 + 12w^2 - 8w + 1)}{(w-1)^6} \right. \\ &\quad \left. \times (-G(0, w) + i\pi) + \frac{(w+1)^3 (7w^2 - 16w + 7)}{(w-1)^5} \right]. \end{aligned} \quad (5.1)$$

And $\Delta_{1,bb}^{C_1C_2}$ reads

$$\begin{aligned} \Delta_{1,bb}^{C_1C_2} &= \frac{m_H m_b \bar{m}_b(\mu)}{v^2\pi} C_A C_F \left[\frac{iw (3w^3 + w^2 + 8w - 5) (\pi + iG(0, w))}{2(w-1)^4} \right. \\ &\quad + \frac{(w+1)^2 (i\pi G(0, w) - 4i\pi G(1, w) - G(0, 0, w) - 2G(0, 1, w) + 4G(1, 0, w) + \pi^2)}{4(w-1)^2} \\ &\quad \left. + \frac{3(w+1)^3}{4(w-1)^3} \left(2G(1, w) + \log \left(\frac{\mu^2}{m_H^2} \right) \right) + \frac{19w^3 + 27w^2 + 27w + 19}{8(w-1)^3} \right], \end{aligned} \quad (5.2)$$

where the factor \bar{m}_b comes from the Yukawa coupling while m_b arises from the propagator due to the requirement of a helicity flip along the fermion line coupled to a Higgs boson.

The higher-order result, $\Delta_{2,bb}^{C_1C_2}$, includes contributions from both the two and four bottom quark final states, as shown in eq. (2.9). The four bottom quark final state contribution is given by

$$\begin{aligned} \Delta_{2,bbbb}^{C_1C_2} &= \frac{m_H m_b \bar{m}_b(\mu)}{v^2} \frac{1}{6912\pi^2 z^2} \left[-3 (279z^2 - 1284z + 1024) F_1^{4b}(z) \right. \\ &\quad + 6 (77z^2 - 764z + 1376) F_2^{4b}(z) + 24(z-4)(71z-172) F_3^{4b}(z) \\ &\quad + 16 (49z^2 - 266z + 256) \beta F_4^{4b}(z) - 24z^2 F_5^{4b}(z) + 48(5z-18)z\beta F_6^{4b}(z) \\ &\quad \left. - 192 (z^2 - 3z - 7) F_7^{4b}(z) - 48(5z-18)z\beta F_8^{4b}(z) - 96 (z^2 - 4z + 2) F_9^{4b}(z) \right], \end{aligned} \quad (5.3)$$

where $\beta = \sqrt{1 - 4/z}$ measures the velocity of the bottom quark and all the color factors $C_F = 4/3$, $C_A = 3$ have been substituted. The complete expressions of all $F_i^{4b}(z)$ can be found in [48]. Their asymptotic expressions in the limit of $z \rightarrow \infty$ are collected in the appendix of ref. [14].

The contribution from the two bottom quark final state is

$$\begin{aligned} \tilde{\Delta}_{2,bb}^{C_1C_2} &= \frac{m_H m_b \bar{m}_b(\mu)}{v^2\pi} \frac{(-w)}{(w-1)^2} \times \\ &\quad \left(\left[\frac{\pi^2 (101w^3 + 99w^2 + 93w + 91)}{6(w-1)w} - \frac{i\pi(w+1)(5w^2 - 2w + 101)}{3(w-1)w} - \frac{(11w^2 - 8w + 11) n_l}{3w} \right. \right. \\ &\quad \left. \left. + \frac{759w^6 - 1586w^5 + 3148w^4 - 3200w^3 + 3148w^2 - 1586w + 759}{6w(w^2 - w + 1)^2} \right] \frac{(w-1)G(-1, w)}{w+1} \right. \\ &\quad \left. + \left[\frac{(17w^4 - 15)\zeta(3)}{3(w-1)} + \frac{i\pi^3 (19w^4 - 108w^3 - 144w^2 - 108w + 19)}{18(w-1)} \right] \right) \end{aligned}$$

$$\begin{aligned}
& + \frac{\pi^2 n_l (w-1)(w+1)^2}{3} + \frac{\pi^2 (379w^4 + 236w^3 - 444w^2 - 84w + 53)}{36(w-1)} \\
& - \frac{i\pi}{72(w-1)^2 (w^2 - w + 1)^3} (8463w^{11} - 33072w^{10} + 69555w^9 - 96715w^8 \\
& + 98026w^7 - 87511w^6 + 76159w^5 - 69754w^4 + 52531w^3 - 29563w^2 + 9664w - 1303) \\
& + \frac{i\pi (23w^3 + 53w^2 + w - 5) n_l}{9} - \frac{1}{144(w-1)(w^2 - w + 1)^2} (2217w^8 - 15298w^7 \\
& - 2595w^6 + 41994w^5 - 102842w^4 + 102798w^3 - 66873w^2 + 18722w - 681) \\
& - \left. \frac{(27w^4 + 64w^3 + 272w^2 - 296w - 21) n_l}{36(w-1)} \right] \frac{G(0, w)}{(w-1)w} \\
& + \left[-\frac{\pi^2 (323w^4 + 48w^3 - 1336w^2 - 192w + 5)}{18(w-1)^2} - \frac{2(w+1)^2 \pi^2 n_l}{9} \right. \\
& + \frac{i\pi}{9(w-1)^2 (w^2 - w + 1)^3} \times (572w^{10} - 2307w^9 + 1796w^8 + 2473w^7 - 11536w^6 \\
& + 15130w^5 - 12130w^4 + 3067w^3 + 1796w^2 - 2505w + 770) \\
& - \frac{i\pi (11w^4 - 214w^2 + 72w + 47) n_l}{9(w-1)^2} + \frac{(15w^2 + 22w + 15)(w+1)n_l}{3(w-1)} \\
& \left. - \frac{(2553w^6 - 674w^5 + 1396w^4 + 3004w^3 + 1396w^2 - 674w + 2553)(w+1)}{24(w-1)(w^2 - w + 1)^2} \right] \frac{G(1, w)}{w} \\
& + \left[(w+1)(5w^2 - 2w + 101) + i\pi(101w^3 + 99w^2 + 93w + 91) \right] \frac{(w+1)G(-1, 0, w)}{3(w-1)^2 w} \\
& + \left[(w-1)(w+1) - i\pi(w^2 + 1) \right] \frac{32(w+1)^2 G(-1, 1, w)}{(w-1)^2 w} \\
& + \left[\frac{(15 - 17w^4) \pi^2}{3} - \frac{2i\pi(w-1)(15w^3 + 31w^2 - 5w - 5)}{3} - \frac{1}{3(w^2 - w + 1)^3} \right. \\
& \times (319w^{10} - 905w^9 + 2704w^8 - 4881w^7 + 7881w^6 - 8794w^5 + 8169w^4 - 5169w^3 \\
& + 2704w^2 - 809w + 223) + \left. \frac{2n_l(3w^4 - 4w^3 + 16w^2 - 4w + 3)}{3} \right] \frac{G(0, -1, w)}{(w-1)^2 w} \\
& + \left[-\frac{\pi^2 (33w^4 - 162w^3 - 216w^2 - 162w + 25)}{18(w-1)^2 w} \right. \\
& + \frac{i\pi (137w^4 + 84w^3 - 162w^2 - 28w + 25)}{12(w-1)^2 w} - \frac{i\pi(w+1)^2 n_l}{3w} - \frac{n_l(23w^3 + 53w^2 + w - 5)}{9(w-1)w} \\
& + \frac{1}{72(w-1)^3 w (w^2 - w + 1)^3} (8463w^{11} - 33072w^{10} + 69555w^9 - 96715w^8 + 98026w^7 \\
& - 87511w^6 + 76159w^5 - 69754w^4 + 52531w^3 - 29563w^2 + 9664w - 1303) G(0, 0, w) \left. \right] \\
& + \left[\frac{\pi^2 (175w^4 - 216w^3 - 288w^2 - 216w - 121)}{9(w-1)^2 w} - \frac{i\pi (98w^4 + 19w^3 - 128w^2 - 5w + 83)}{3(w-1)^2 w} \right. \\
& + \left. \frac{2i\pi(w+1)^2 n_l}{3w} - \frac{(37w^3 + 61w^2 + 47w - 1) n_l}{9(w-1)w} + \frac{1}{12(w-1)^2 w (w^2 - w + 1)^3} \right]
\end{aligned}$$

$$\begin{aligned}
& \times (271w^{10} - 1053w^9 + 1754w^8 - 2365w^7 + 2041w^6 - 2702w^5 \\
& + 2833w^4 - 3157w^3 + 1754w^2 - 789w + 7) \Big] G(0, 1, w) \\
& + \left[12(w-1)(w+1)^3 - i\pi(11w^4 + 20w^3 + 34w^2 + 20w + 11) \right] \frac{8G(1, -1, w)}{3(w-1)^2w} \\
& + \left[-3i\pi(157w^4 - 28w^3 - 734w^2 - 156w - 7) + 2(11w^4 - 214w^2 + 72w + 47)n_l \right. \\
& - \frac{2}{(w^2 - w + 1)^3} (572w^{10} - 2307w^9 + 1796w^8 + 2473w^7 - 11536w^6 + 15130w^5 \\
& - 12130w^4 + 3067w^3 + 1796w^2 - 2505w + 770) \Big] \frac{G(1, 0, w)}{18(w-1)^2w} \\
& + \left[\frac{3i\pi(19w^4 - 60w^3 - 174w^2 - 60w + 19)}{2(w-1)} - 4i\pi(w-1)(w+1)^2n_l \right. \\
& - 81(w+1)^3 + 6n_l(w+1)^3 \Big] \frac{2G(1, 1, w)}{3(w-1)w} \\
& - \frac{(w+1)(101w^3 + 99w^2 + 93w + 91)G(-1, 0, 0, w)}{3(w-1)^2w} \\
& + \left[(w-1)(15w^3 + 31w^2 - 5w - 5) - i\pi(17w^4 - 15) \right] \frac{2G(0, -1, 0, w)}{3(w-1)^2w} \\
& + \left[2i\pi(5w^4 - 3) - 29w^4 + 105w^3 + 31w^2 + 105w - 29 \right. \\
& + 2(w-1)^2(w+1)^2n_l \Big] \frac{2G(0, 0, -1, w)}{3(w-1)^2w} \\
& + \left[-4i\pi(7w^4 - 27w^3 - 36w^2 - 27w + 3) - 137w^4 - 84w^3 + 162w^2 + 28w - 25 \right. \\
& + 4(w-1)^2(w+1)^2n_l \Big] \frac{G(0, 0, 0, w)}{12(w-1)^2w} \\
& + \left[6i\pi(17w^4 - 15) - 117w^4 + 146w^3 + 110w^2 + 242w - 15 \right. \\
& + 4(w-1)^2(w+1)^2n_l \Big] \frac{G(0, 0, 1, w)}{6(w-1)^2w} \\
& + \left[2i\pi(37w^4 - 54w^3 - 72w^2 - 54w - 23) + 98w^4 + 19w^3 - 128w^2 + 2 - 5w + 83 \right. \\
& - 2(w-1)^2(w+1)^2n_l \Big] \frac{G(0, 1, 0, w)}{3(w-1)^2w} \\
& + \left[32i\pi(w-1)(w^2+1)(w+1) - 2(19w^2 + 58w + 19)(w+1)^2 \right. \\
& - 4(w-1)^2(w+1)^2n_l \Big] \frac{G(0, 1, 1, w)}{3(w-1)^2w} + \frac{8(11w^4 + 20w^3 + 34w^2 + 20w + 11)G(1, -1, 0, w)}{3(w-1)^2w} \\
& + \left[-8(w-1)^2(w+1)^2n_l - 16(5w^4 + 15w^3 + 8w^2 + 15w + 5) \right] \frac{G(1, 0, -1, w)}{3(w-1)^2w}
\end{aligned}$$

$$\begin{aligned}
& + \frac{(157w^4 - 28w^3 - 734w^2 - 156w - 7)G(1, 0, 0, w)}{6(w-1)^2w} - \frac{2(13w^2 + 30w + 13)G(1, 0, 1, w)}{3w} \\
& + \left[-3(19w^4 - 60w^3 - 174w^2 - 60w + 19) + 8(w-1)^2(w+1)^2n_l \right] \frac{G(1, 1, 0, w)}{3(w-1)^2w} \\
& - \frac{4(5w^4 - 3)G(0, 0, -1, 0, w)}{3(w-1)^2w} + \frac{(7w^4 - 27w^3 - 36w^2 - 27w + 3)G(0, 0, 0, 0, w)}{3(w-1)^2w} \\
& + \frac{(29w^4 - 54w^3 - 72w^2 - 54w - 11)G(0, 0, 0, 1, w)}{3(w-1)^2w} \\
& - \frac{2(37w^4 - 54w^3 - 72w^2 - 54w - 23)G(0, 1, 0, 0, w)}{3(w-1)^2w} \\
& + \frac{(17w^4 - 15)}{3(w-1)^2w} \left[2G(0, -1, 0, 0, w) - 3G(0, 0, 1, 0, w) \right] \\
& + \frac{27w^4 + w^3 + 11w^2 + w + 27}{9(w-1)^2w} \left[8\pi^2G(x_1, w) + 12i\pi G(x_1, 0, w) + 3i\pi G(x_1, 1, w) \right. \\
& + 18G(x_1, 0, -1, w) - 12G(x_1, 0, 0, w) + 9G(x_1, 0, 1, w) - 3G(x_1, 1, 0, w) \\
& + 8\pi^2G(x_2, w) + 12i\pi G(x_2, 0, w) + 3i\pi G(x_2, 1, w) + 18G(x_2, 0, -1, w) \\
& \left. - 12G(x_2, 0, 0, w) + 9G(x_2, 0, 1, w) - 3G(x_2, 1, 0, w) \right] \\
& - \frac{8(w+1)}{3(w-1)^2w} \left[8\pi^2G(0, x_1, w)w^3 + 8\pi^2G(0, x_2, w)w^3 - 12G(-1, 0, 1, w)w^3 \right. \\
& - 12G(-1, 1, 0, w)w^3 - 4i\pi G(0, -1, 1, w)w^3 + 16G(0, -1, 1, w)w^3 \\
& - 4i\pi G(0, 1, -1, w)w^3 + 16G(0, 1, -1, w)w^3 + 12i\pi G(0, x_1, 0, w)w^3 \\
& + 3i\pi G(0, x_1, 1, w)w^3 + 12i\pi G(0, x_2, 0, w)w^3 + 3i\pi G(0, x_2, 1, w)w^3 \\
& + 4G(0, -1, 0, 1, w)w^3 + 4G(0, -1, 1, 0, w)w^3 - 8G(0, 0, -1, 1, w)w^3 \\
& - 4G(0, 0, 0, -1, w)w^3 - 8G(0, 0, 1, -1, w)w^3 - 6G(0, 0, 1, 1, w)w^3 \\
& + 4G(0, 1, -1, 0, w)w^3 - 20G(0, 1, 0, -1, w)w^3 - 3G(0, 1, 0, 1, w)w^3 \\
& + 4G(0, 1, 1, 0, w)w^3 + 18G(0, x_1, 0, -1, w)w^3 - 12G(0, x_1, 0, 0, w)w^3 \\
& + 9G(0, x_1, 0, 1, w)w^3 - 3G(0, x_1, 1, 0, w)w^3 + 18G(0, x_2, 0, -1, w)w^3 \\
& - 12G(0, x_2, 0, 0, w)w^3 + 9G(0, x_2, 0, 1, w)w^3 - 3G(0, x_2, 1, 0, w)w^3 \\
& - 8\pi^2G(0, x_1, w)w^2 - 8\pi^2G(0, x_2, w)w^2 - 12G(-1, 0, 1, w)w^2 \\
& - 12G(-1, 1, 0, w)w^2 + 4i\pi G(0, -1, 1, w)w^2 + 8G(0, -1, 1, w)w^2 \\
& + 4i\pi G(0, 1, -1, w)w^2 + 8G(0, 1, -1, w)w^2 - 12i\pi G(0, x_1, 0, w)w^2 \\
& - 3i\pi G(0, x_1, 1, w)w^2 - 12i\pi G(0, x_2, 0, w)w^2 - 3i\pi G(0, x_2, 1, w)w^2 \\
& - 4G(0, -1, 0, 1, w)w^2 - 4G(0, -1, 1, 0, w)w^2 + 8G(0, 0, -1, 1, w)w^2 \\
& + 4G(0, 0, 0, -1, w)w^2 + 8G(0, 0, 1, -1, w)w^2 + 6G(0, 0, 1, 1, w)w^2 \\
& - 4G(0, 1, -1, 0, w)w^2 + 20G(0, 1, 0, -1, w)w^2 + 3G(0, 1, 0, 1, w)w^2 \\
& - 4G(0, 1, 1, 0, w)w^2 - 18G(0, x_1, 0, -1, w)w^2 + 12G(0, x_1, 0, 0, w)w^2 \\
& \left. - 9G(0, x_1, 0, 1, w)w^2 + 3G(0, x_1, 1, 0, w)w^2 - 18G(0, x_2, 0, -1, w)w^2 \right]
\end{aligned}$$

$$\begin{aligned}
& + 12G(0, x_2, 0, 0, w)w^2 - 9G(0, x_2, 0, 1, w)w^2 + 3G(0, x_2, 1, 0, w)w^2 \\
& + 8\pi^2G(0, x_1, w)w + 8\pi^2G(0, x_2, w)w - 12G(-1, 0, 1, w)w \\
& - 12G(-1, 1, 0, w)w - 4i\pi G(0, -1, 1, w)w + 8G(0, -1, 1, w)w \\
& - 4i\pi G(0, 1, -1, w)w + 8G(0, 1, -1, w)w + 12i\pi G(0, x_1, 0, w)w \\
& + 3i\pi G(0, x_1, 1, w)w + 12i\pi G(0, x_2, 0, w)w + 3i\pi G(0, x_2, 1, w)w \\
& + 4G(0, -1, 0, 1, w)w + 4G(0, -1, 1, 0, w)w - 8G(0, 0, -1, 1, w)w \\
& - 4G(0, 0, 0, -1, w)w - 8G(0, 0, 1, -1, w)w - 6G(0, 0, 1, 1, w)w \\
& + 4G(0, 1, -1, 0, w)w - 20G(0, 1, 0, -1, w)w - 3G(0, 1, 0, 1, w)w \\
& + 4G(0, 1, 1, 0, w)w + 18G(0, x_1, 0, -1, w)w - 12G(0, x_1, 0, 0, w)w \\
& + 9G(0, x_1, 0, 1, w)w - 3G(0, x_1, 1, 0, w)w + 18G(0, x_2, 0, -1, w)w \\
& - 12G(0, x_2, 0, 0, w)w + 9G(0, x_2, 0, 1, w)w - 3G(0, x_2, 1, 0, w)w \\
& - 8\pi^2G(0, x_1, w) - 8\pi^2G(0, x_2, w) - 12G(-1, 0, 1, w) \\
& - 12G(-1, 1, 0, w) + 4i\pi G(0, -1, 1, w) + 16G(0, -1, 1, w) \\
& + 4i\pi G(0, 1, -1, w) + 16G(0, 1, -1, w) - 12i\pi G(0, x_1, 0, w) \\
& - 3i\pi G(0, x_1, 1, w) - 12i\pi G(0, x_2, 0, w) - 3i\pi G(0, x_2, 1, w) \\
& - 4G(0, -1, 0, 1, w) - 4G(0, -1, 1, 0, w) + 8G(0, 0, -1, 1, w) \\
& + 4G(0, 0, 0, -1, w) + 8G(0, 0, 1, -1, w) + 6G(0, 0, 1, 1, w) \\
& - 4G(0, 1, -1, 0, w) + 20G(0, 1, 0, -1, w) + 3G(0, 1, 0, 1, w) \\
& - 4G(0, 1, 1, 0, w) - 18G(0, x_1, 0, -1, w) + 12G(0, x_1, 0, 0, w) \\
& - 9G(0, x_1, 0, 1, w) + 3G(0, x_1, 1, 0, w) - 18G(0, x_2, 0, -1, w) \\
& + 12G(0, x_2, 0, 0, w) - 9G(0, x_2, 0, 1, w) + 3G(0, x_2, 1, 0, w) \Big] \\
& + \left[\frac{\pi^4 (141w^4 - 1080w^3 - 1440w^2 - 1080w + 253)}{360(w-1)^2w} - \frac{i\pi (17w^4 - 15)\zeta(3)}{3(w-1)^2w} \right. \\
& - \frac{(62w^4 - 93w^3 + 42w^2 + 55w + 135)\zeta(3)}{3(w-1)^2w} + \frac{4(w+1)^2\zeta(3)n_l}{3w} \\
& - \frac{i\pi^3 (121w^4 + 76w^3 - 141w^2 - 28w + 14)}{18(w-1)^2w} + \frac{2i\pi^3(w+1)^2n_l}{9w} \\
& - \frac{\pi^2}{216(w-1)^3w(w^2-w+1)^3} (18781w^{11} - 75856w^{10} + 168361w^9 - 254009w^8 \\
& + 290798w^7 - 291965w^6 + 268037w^5 - 232550w^4 + 164321w^3 - 88657w^2 \\
& + 29512w - 4837) + \frac{\pi^2 (43w^4 + 38w^3 - 58w^2 - 22w + 13)n_l}{18(w-1)^2w} \\
& + \frac{i\pi}{144(w-1)^2w(w^2-w+1)^2} (2217w^8 - 15298w^7 - 2595w^6 + 41994w^5 - 102842w^4 \\
& + 102798w^3 - 66873w^2 + 18722w - 681) + \frac{i\pi (27w^4 + 64w^3 + 272w^2 - 296w - 21)n_l}{36(w-1)^2w}
\end{aligned}$$

$$- \frac{(w+1)(21609w^2 + 6184w + 21609)}{96(w-1)w} + \frac{(w+1)(308w^2 + w + 308)n_l}{36(w-1)w} \Big] \Big) \quad (5.4)$$

with $x_1 = l_4^{\text{NP1}}$ and $x_2 = l_5^{\text{NP1}}$. For simplicity, the color factors $C_F = 4/3$, $C_A = 3$, $T_R = 1/2$ and $\mu = m_H$ have been substituted. Note that the above result is real, although there are $i\pi$ factors in some terms. The imaginary part of the G function can be fixed by assigning $w + i0^+$. We also provide the analytical results in the auxiliary files submitted along this paper.

6 Asymptotic expansion

6.1 Small m_b limit of $\Gamma_{H \rightarrow b\bar{b}}$

With the full analytical expressions at hand, it is interesting to study the asymptotic behaviors of $\Delta_{b\bar{b}}^{i,C_1C_1}$ and $\Delta_{i,b\bar{b}}^{C_1C_2}$. Firstly we consider the limit of $z \rightarrow \infty$, corresponding to $m_b \rightarrow 0$. $\Delta_{1,b\bar{b}}^{C_1C_1}$ in this limit is given by

$$\Delta_{1,b\bar{b}}^{C_1C_1}|_{z \rightarrow \infty} = \frac{m_H^3}{\pi v^2} C_A C_F \left[\frac{1}{6} \log(z) - \frac{7}{12} + \frac{3}{z} \right] + \mathcal{O}(z^{-2}). \quad (6.1)$$

The logarithm embodies the collinear divergence of a gluon splitting to a bottom quark pair in the massless limit. The bottom quark mass serves as a regulator. If one considers the decay to massless bottom quarks, the decay rate is divergent, and thus the decay width of a Higgs boson to massless bottom quarks is not well defined. In such cases, one has to consider the decay to all partons.

The interference contribution in the small mass limit becomes

$$\begin{aligned} \Delta_{1,b\bar{b}}^{C_1C_2}|_{z \rightarrow \infty} &= \frac{m_H m_b \bar{m}_b(\mu)}{\pi v^2} C_A C_F \left[-\frac{1}{8} \log^2(z) - \frac{3}{4} \log\left(\frac{\mu^2}{m_H^2}\right) + \frac{\pi^2}{8} - \frac{19}{8} \right. \\ &\quad \left. + \frac{1}{2} \frac{\log^2(z)}{z} + 2 \frac{\log(z)}{z} + \frac{9}{2z} \log\left(\frac{\mu^2}{m_H^2}\right) - \frac{\pi^2}{2z} + \frac{15}{2z} \right] + \mathcal{O}(z^{-2}), \end{aligned} \quad (6.2)$$

where the double logarithm dominates the contribution over the other terms. This kind of double logarithm is induced by soft massive quarks. It differs from the traditional Sudakov double logarithm, which is induced by soft gluons. The all-order structure of this double logarithm is still unclear. Similar double logarithms appear in the result of the $H \rightarrow \gamma\gamma$ decay via a bottom quark loop, and resummation of the double logarithms to all orders has been realized in diagrammatic analyses [64, 65] or soft-collinear effective theory [66, 67]. However, the methods can not be directly applied here because the corrections of real emissions, which are not needed in $H \rightarrow \gamma\gamma$, have to be included. We leave such an interesting topic to future work. Below we present the higher-order corrections,

$$\begin{aligned} \tilde{\Delta}_{2,b\bar{b}}^{C_1C_2}|_{z \rightarrow \infty} &= \frac{m_H m_b \bar{m}_b(\mu)}{\pi v^2} \times \\ &\left(C_A^2 C_F \left[-\frac{1}{96} \log^4(z) + \frac{5}{288} \log^3(z) + \frac{\pi^2}{24} \log^2(z) - \frac{11}{48} \log\left(\frac{\mu^2}{m_H^2}\right) \log^2(z) \right. \right. \end{aligned}$$

$$\begin{aligned}
& -\frac{601}{576} \log^2(z) + \frac{\zeta(3)}{4} \log(z) + \frac{7\pi^2}{96} \log(z) + \frac{125}{192} \log(z) - \frac{11}{16} \log^2\left(\frac{\mu^2}{m_H^2}\right) \\
& + \frac{11\pi^2}{48} \log\left(\frac{\mu^2}{m_H^2}\right) - \frac{51}{8} \log\left(\frac{\mu^2}{m_H^2}\right) - \frac{\pi^4}{40} + \frac{25\zeta(3)}{12} + \frac{673\pi^2}{576} - \frac{19225}{1152} \\
& + \frac{1}{96} \frac{\log^4(z)}{z} + \frac{2}{9} \frac{\log^3(z)}{z} + \frac{11}{12} \log\left(\frac{\mu^2}{m_H^2}\right) \frac{\log^2(z)}{z} + \frac{\pi^2 \log^2(z)}{48z} - \zeta(3) \frac{\log(z)}{z} \\
& - \frac{13\pi^2 \log(z)}{12z} + \frac{103 \log^2(z)}{36z} + \frac{11}{3} \log\left(\frac{\mu^2}{m_H^2}\right) \frac{\log(z)}{z} + \frac{82 \log(z)}{9z} \\
& + \frac{33}{8z} \log^2\left(\frac{\mu^2}{m_H^2}\right) - \frac{11\pi^2}{12z} \log\left(\frac{\mu^2}{m_H^2}\right) + \frac{207}{8z} \log\left(\frac{\mu^2}{m_H^2}\right) + \frac{11\pi^4}{160z} \\
& - \frac{55\zeta(3)}{12z} - \frac{185\pi^2}{72z} + \frac{4001}{96z}] \\
& + C_A C_F^2 \left[\frac{1}{64} \log^4(z) - \frac{5}{32} \log^3(z) - \frac{3}{32} \log\left(\frac{\mu^2}{m_H^2}\right) \log^2(z) - \frac{\pi^2}{96} \log^2(z) + \frac{3}{4} \log^2(z) \right. \\
& - \frac{3\zeta(3)}{2} \log(z) - \frac{\pi^2}{96} \log(z) + \frac{9}{16} \log\left(\frac{\mu^2}{m_H^2}\right) \log(z) - \frac{23}{32} \log(z) - \frac{9}{16} \log^2\left(\frac{\mu^2}{m_H^2}\right) \\
& + \frac{3\pi^2}{32} \log\left(\frac{\mu^2}{m_H^2}\right) - \frac{141}{32} \log\left(\frac{\mu^2}{m_H^2}\right) + \frac{\pi^4}{64} + \frac{15\zeta(3)}{4} - \frac{\pi^2}{6} - \frac{427}{64} \\
& - \frac{1}{16} \frac{\log^4(z)}{z} - \frac{1}{24} \frac{\log^3(z)}{z} + \frac{\pi^2 \log^2(z)}{24z} + \frac{3}{8} \log\left(\frac{\mu^2}{m_H^2}\right) \frac{\log^2(z)}{z} - \frac{33 \log^2(z)}{8z} \\
& + 6\zeta(3) \frac{\log(z)}{z} + \frac{41\pi^2 \log(z)}{24z} - \frac{69}{8} \log\left(\frac{\mu^2}{m_H^2}\right) \frac{\log(z)}{z} - \frac{9 \log(z)}{2z} + \frac{27}{8z} \log^2\left(\frac{\mu^2}{m_H^2}\right) \\
& \left. - \frac{3\pi^2}{8z} \log\left(\frac{\mu^2}{m_H^2}\right) + \frac{63}{4z} \log\left(\frac{\mu^2}{m_H^2}\right) - \frac{\pi^4}{16z} - \frac{25\zeta(3)}{z} - \frac{43\pi^2}{24z} + \frac{979}{32z} \right] \\
& + C_A C_F n_l \left[\frac{1}{72} \log^3(z) + \frac{5}{72} \log^2(z) - \frac{\pi^2}{24} \log(z) + \frac{1}{24} \log\left(\frac{\mu^2}{m_H^2}\right) \log^2(z) \right. \\
& + \frac{7}{48} \log(z) + \frac{1}{8} \log^2\left(\frac{\mu^2}{m_H^2}\right) - \frac{\pi^2}{24} \log\left(\frac{\mu^2}{m_H^2}\right) + \log\left(\frac{\mu^2}{m_H^2}\right) - \frac{\zeta(3)}{3} - \frac{\pi^2}{9} + \frac{77}{36} \\
& - \frac{1}{18} \frac{\log^3(z)}{z} - \frac{1}{6} \log\left(\frac{\mu^2}{m_H^2}\right) \frac{\log^2(z)}{z} - \frac{5 \log^2(z)}{18z} + \frac{\pi^2 \log(z)}{6z} \\
& - \frac{2}{3} \log\left(\frac{\mu^2}{m_H^2}\right) \frac{\log(z)}{z} - \frac{16 \log(z)}{9z} + \frac{\pi^2}{6z} \log\left(\frac{\mu^2}{m_H^2}\right) - \frac{3}{4z} \log^2\left(\frac{\mu^2}{m_H^2}\right) \\
& \left. - \frac{15}{4z} \log\left(\frac{\mu^2}{m_H^2}\right) + \frac{4\zeta(3)}{3z} + \frac{13\pi^2}{36z} - \frac{241}{48z} \right] \\
& + C_A C_F \left[\frac{5}{72} \log^3(z) + \frac{1}{24} \log\left(\frac{\mu^2}{m_H^2}\right) \log^2(z) - \frac{19}{144} \log^2(z) - \frac{7\pi^2}{72} \log(z) \right. \\
& + \frac{3}{16} \log(z) + \frac{1}{8} \log^2\left(\frac{\mu^2}{m_H^2}\right) - \frac{\pi^2}{24} \log\left(\frac{\mu^2}{m_H^2}\right) + \log\left(\frac{\mu^2}{m_H^2}\right) + \frac{23\pi^2}{432} + \frac{43}{16} \\
& \left. - \frac{5 \log^3(z)}{18z} - \frac{1}{6} \log\left(\frac{\mu^2}{m_H^2}\right) \frac{\log^2(z)}{z} + \frac{4 \log^2(z)}{9z} + \frac{7\pi^2 \log(z)}{18z} \right]
\end{aligned}$$

$$\begin{aligned}
& -\frac{2}{3} \log\left(\frac{\mu^2}{m_H^2}\right) \frac{\log(z)}{z} - \frac{101 \log(z)}{36z} - \frac{3}{4z} \log^2\left(\frac{\mu^2}{m_H^2}\right) + \frac{\pi^2}{6z} \log\left(\frac{\mu^2}{m_H^2}\right) \\
& - \frac{15}{4z} \log\left(\frac{\mu^2}{m_H^2}\right) - \frac{65\pi^2}{108z} - \frac{1811}{144z} \Big] + \mathcal{O}(z^{-2})
\end{aligned} \tag{6.3}$$

and

$$\begin{aligned}
\Delta_{2,bbbb}^{C_1 C_2}|_{z \rightarrow \infty} &= \frac{m_H m_b \overline{m}_b(\mu)}{\pi v^2} \times \\
& \left((C_A^2 C_F - 2C_A C_F^2) \left[\frac{1}{192} \log^4(z) - \frac{1}{16} \log^3(z) - \frac{\pi^2}{96} \log^2(z) + \frac{7}{16} \log^2(z) \right. \right. \\
& + \frac{\pi^2}{16} \log(z) - \frac{5}{4} \log(z) - \frac{\zeta(3)}{4} \log(z) + \frac{19\pi^4}{960} + \frac{7\zeta(3)}{8} - \frac{\pi^2}{3} + \frac{23}{16} \\
& - \frac{1}{48} \frac{\log^4(z)}{z} + \frac{1}{6} \frac{\log^3(z)}{z} + \frac{\pi^2}{24} \frac{\log^2(z)}{z} - \frac{13}{8} \frac{\log^2(z)}{z} + \zeta(3) \frac{\log(z)}{z} - \frac{\pi^2}{12} \frac{\log(z)}{z} \\
& \left. + \frac{9}{2} \frac{\log(z)}{z} - \frac{19\pi^4}{240z} - \frac{9\zeta(3)}{2z} + \frac{7\pi^2}{8z} - \frac{7}{2z} \right] \\
& + C_A C_F \left[-\frac{1}{36} \log^3(z) + \frac{19}{144} \log^2(z) + \frac{\pi^2}{18} \log(z) - \frac{17}{48} \log(z) - \frac{\zeta(3)}{2} - \frac{41\pi^2}{432} + \frac{25}{96} \right. \\
& \left. + \frac{1}{9} \frac{\log^3(z)}{z} - \frac{11}{18} \frac{\log^2(z)}{z} - \frac{2\pi^2}{9} \frac{\log(z)}{z} + \frac{31}{18} \frac{\log(z)}{z} + \frac{2\zeta(3)}{z} + \frac{37\pi^2}{54z} + \frac{25}{18z} \right] \Big) + \mathcal{O}(z^{-2}),
\end{aligned} \tag{6.4}$$

for the two and four bottom quark final states, respectively. Both contributions exhibit double logarithmic enhancement, i.e., the $\alpha_s^n \log^{2n}(z)$ expansion pattern. These terms break the perturbative convergence of the higher-order corrections and have to be resummed to all orders to provide reliable theoretical predictions. The above analytic results can be used to check the consistency of the resummation formula in the future.

Combining the two corrections in eq. (6.3) and eq. (6.4), we get the leading logarithm of $\Delta_{2,b\bar{b}}^{C_1 C_2}$,

$$-\frac{m_H m_b \overline{m}_b(\mu)}{8\pi v^2} C_A C_F \log^2(z) \times \frac{1}{24} (C_A - C_F) \log^2(z). \tag{6.5}$$

This color structure distinguishes it from the Sudakov double logarithms and shares the same features as the results for the quark-gluon splitting function [68], $Hb\bar{b}/Hgg$ form factors [65, 69], and off-diagonal ‘‘gluon’’ thrust [70–72].

To provide the full $\mathcal{O}(\alpha_s^3)$ corrections, we also need the analytical expression of the third order correction in $\Gamma_{H \rightarrow b\bar{b}}^{C_2 C_2}$ [18–21],

$$\begin{aligned}
\Delta_{3,b\bar{b}}^{C_2 C_2}|_{z \rightarrow \infty} &= \frac{m_H \overline{m}_b(\mu)^2}{512v^2\pi} C_A \times \\
& \left(C_A C_F^2 \left[\frac{100\zeta(5)}{3} - \frac{4658\zeta(3)}{3} - \frac{3430\pi^2}{27} + \frac{3894493}{972} \right] \right. \\
& \left. + C_A^2 C_F \left[580\zeta(5) - 2178\zeta(3) - \frac{766\pi^2}{3} + \frac{13153}{3} \right] \right)
\end{aligned}$$

$$\begin{aligned}
& + C_F^3 \left[360\zeta(5) - 956\zeta(3) - 108\pi^2 + \frac{23443}{12} \right] \\
& + C_A C_F n_f \left[-\frac{80\zeta(5)}{3} + \frac{4\pi^4}{15} - \frac{704\zeta(3)}{3} - \frac{1142\pi^2}{27} + \frac{267800}{243} \right] \\
& + C_F^2 n_f \left[160\zeta(5) - \frac{4\pi^4}{15} - 520\zeta(3) - \frac{130\pi^2}{3} + \frac{2816}{3} \right] \\
& + C_F n_f^2 \left[-16\zeta(3) - \frac{88\pi^2}{27} + \frac{15511}{243} \right] \Big) + \mathcal{O}(z^{-1}), \tag{6.6}
\end{aligned}$$

where $\mu = m_H$ have been substituted. We see that there is no logarithmic enhancement in this part. The $\mathcal{O}(z^{-1})$ term has been computed at α_s^2 in [14–16], and is found to be less than 1% of the $\mathcal{O}(z^0)$ contribution. The result of $\mathcal{O}(z^{-1})$ term at α_s^3 is expected to be also a few percent of the $\mathcal{O}(z^0)$ term at this order, and thus completely negligible.

Combining all the above expressions with the Wilson coefficients in eq. (2.5), and converting the on-shell m_b to \overline{m}_b in the $\overline{\text{MS}}$ scheme via the relation

$$\overline{m}_b(\mu) = m_b \left(1 - \left(\frac{\alpha_s}{\pi} \right) C_F \left[1 + \frac{3}{4} \log \left(\frac{\mu^2}{m_b^2} \right) \right] + \mathcal{O}(\alpha_s^2) \right), \tag{6.7}$$

we obtain a compact result of $\Gamma_{H \rightarrow b\bar{b}}$ up to $\mathcal{O}(\alpha_s^3)$,

$$\begin{aligned}
\Gamma_{H \rightarrow b\bar{b}} = & \frac{3m_H \overline{m}_b^2}{8v^2\pi} \left\{ 1 + \left(\frac{\alpha_s}{\pi} \right) \frac{17}{3} \right. \\
& + \left(\frac{\alpha_s}{\pi} \right)^2 \left[\frac{1}{9} \log^2(\bar{z}) - \frac{2}{3} \log(x) - \frac{97\zeta(3)}{6} - \frac{17\pi^2}{12} + \frac{9235}{144} \right] \\
& + \left(\frac{\alpha_s}{\pi} \right)^3 \left[\frac{5}{648} \log^4(\bar{z}) + \frac{59}{324} \log^3(\bar{z}) - \frac{31\pi^2}{324} \log^2(\bar{z}) + \frac{989}{648} \log^2(\bar{z}) \right. \\
& + \frac{32\zeta(3)}{27} \log(\bar{z}) - \frac{41\pi^2}{324} \log(\bar{z}) + \frac{137}{216} \log(\bar{z}) - \frac{23}{18} \log^2(x) - \frac{49}{6} \log(x) \\
& + \left. \frac{1945\zeta(5)}{36} - \frac{13\pi^4}{3240} - \frac{81239\zeta(3)}{216} - \frac{81239\zeta(3)}{216} - \frac{22291\pi^2}{648} + \frac{37434709}{46656} \right] \Big\} \\
& + \frac{m_H^3}{v^2\pi} \left(\frac{\alpha_s}{\pi} \right)^3 \left[\frac{\log(\bar{z})}{216} - \frac{7}{432} \right] + \mathcal{O}(\bar{z}^{-1}) + \mathcal{O}(x) + \mathcal{O}(\alpha_s^4) \tag{6.8}
\end{aligned}$$

with $\bar{z} = m_H^2/\overline{m}_b^2$ and $x = m_H^2/m_t^2$. The color factors $C_F = 4/3$, $C_A = 3$, $T_R = 1/2$, $n_f = 5$, $n_l = 4$ and $\mu = m_H$ have been applied after we checked the scale independence of the expression up to $\mathcal{O}(\alpha_s^3)$. The above expression up to $\mathcal{O}(\alpha_s^2)$ agrees with the results in [15, 73]. The $\mathcal{O}(\alpha_s^3)$ correction is new. The large logarithmic terms, $\log^i(\bar{z})$, $i = 1, \dots, 4$, in the curly bracket provide significant corrections to the decay width. The last term in the above equation is of order α_s^3 , but is power enhanced by $\bar{z} \log(\bar{z})$ compared to the LO decay width. If this term dominates the contribution, it would be hard to extract the value of bottom quark mass from the decay width because of its logarithmic dependence on m_b . Fortunately, due to the small coefficient, this term does not play a significant role.

We also calculate the partial decay width of $\Gamma_{H \rightarrow gg}$ in the small m_b limit explicitly in a similar way, and the result is given by

$$\Gamma_{H \rightarrow gg} = \frac{m_H \overline{m}_b^2}{v^2\pi} \left\{ \left(\frac{\alpha_s}{\pi} \right)^2 \left[-\frac{1}{24} \log^2(\bar{z}) + \frac{\pi^2}{24} + \frac{1}{6} \right] \right.$$

$$\begin{aligned}
& + \left(\frac{\alpha_s}{\pi}\right)^3 \left[-\frac{5}{1728} \log^4(\bar{z}) - \frac{59}{864} \log^3(\bar{z}) + \frac{31\pi^2}{864} \log^2(\bar{z}) - \frac{989}{1728} \log^2(\bar{z}) \right. \\
& - \frac{4\zeta(3)}{9} \log(\bar{z}) + \frac{41\pi^2}{864} \log(\bar{z}) - \frac{137}{576} \log(\bar{z}) - \frac{137\pi^4}{8640} - \frac{29\zeta(3)}{36} \\
& \left. + \frac{1277\pi^2}{1728} + \frac{17275}{3456} \right] \Big\} + \frac{m_H^3}{v^2\pi} \left\{ \left(\frac{\alpha_s}{\pi}\right)^2 \frac{1}{72} + \left(\frac{\alpha_s}{\pi}\right)^3 \left[-\frac{1}{216} \log(\bar{z}) + \frac{229}{864} \right] \right\} \\
& + \mathcal{O}(\bar{z}^{-1}) + \mathcal{O}(x) + \mathcal{O}(\alpha_s^4). \tag{6.9}
\end{aligned}$$

Similar large logarithmic/power enhancements are observed.

Summing up the above two contributions, we obtain the decay width of the Higgs boson to all hadrons,

$$\begin{aligned}
\Gamma_{H \rightarrow \text{hadrons}} &= \frac{3m_H \bar{m}_b^2}{8v^2\pi} \left\{ 1 + \left(\frac{\alpha_s}{\pi}\right) \frac{17}{3} + \left(\frac{\alpha_s}{\pi}\right)^2 \left[-\frac{2}{3} \log(x) - \frac{97\zeta(3)}{6} - \frac{47\pi^2}{36} + \frac{9299}{144} \right] \right. \\
& + \left(\frac{\alpha_s}{\pi}\right)^3 \left[-\frac{23}{18} \log^2(x) - \frac{49}{6} \log(x) + \frac{1945\zeta(5)}{36} - \frac{5\pi^4}{108} - \frac{81703\zeta(3)}{216} \right. \\
& \left. \left. - \frac{10507\pi^2}{324} + \frac{38056609}{46656} \right] \right\} + \frac{m_H^3}{v^2\pi} \left\{ \left(\frac{\alpha_s}{\pi}\right)^2 \frac{1}{72} + \left(\frac{\alpha_s}{\pi}\right)^3 \frac{215}{864} \right\} \\
& + \mathcal{O}(\bar{z}^{-1}) + \mathcal{O}(x) + \mathcal{O}(\alpha_s^4). \tag{6.10}
\end{aligned}$$

The above result coincides with that in refs. [34, 35] obtained in a different method. This is a strong check of our calculation.

6.2 Threshold limit

It is also interesting to investigate the threshold limit of bottom quark pair production. Expanding the full analytic results in the limit of $m_H \rightarrow 2m_b$ or $\beta \rightarrow 0$, we have

$$\Delta_{1,bb}^{C_1 C_1} |_{\beta \rightarrow 0} = \frac{m_H^3}{\pi v^2} C_A C_F \frac{4}{315} \beta^9 + \mathcal{O}(\beta^{10}) \tag{6.11}$$

and

$$\Delta_{1,bb}^{C_1 C_2} |_{\beta \rightarrow 0} = \frac{m_H m_b \bar{m}_b(\mu)}{\pi v^2} C_A C_F \left[-\frac{3}{4} \log\left(\frac{\mu^2}{m_H^2}\right) - \frac{\log(2)}{2} - 1 \right] \beta^3 + \mathcal{O}(\beta^4). \tag{6.12}$$

It can be seen that the contribution from the \mathcal{O}_1 operator is highly suppressed near the threshold. For comparison, we also present the result of $\Delta_{1,bb}^{C_2 C_2}$,

$$\Delta_{1,bb}^{C_2 C_2} |_{\beta \rightarrow 0} = \frac{m_H \bar{m}_b(\mu)^2}{\pi v^2} C_A C_F \frac{\pi^2}{16} \beta^2 + \mathcal{O}(\beta^3), \tag{6.13}$$

which is $1/\beta$ power enhanced with respect to the LO result due to Coulomb interaction between the bottom quark pair. The NLO result of $\Delta_{bb}^{C_1 C_2}$ in the threshold limit is given by

$$\Delta_{2,bb}^{C_1 C_2} |_{\beta \rightarrow 0} = \frac{m_H m_b \bar{m}_b(\mu)}{\pi v^2} \left(C_A C_F^2 \beta^2 \pi^2 \left[-\frac{3}{8} \log\left(\frac{\mu^2}{m_H^2}\right) - \frac{\log(2)}{4} - \frac{1}{2} \right] \right)$$

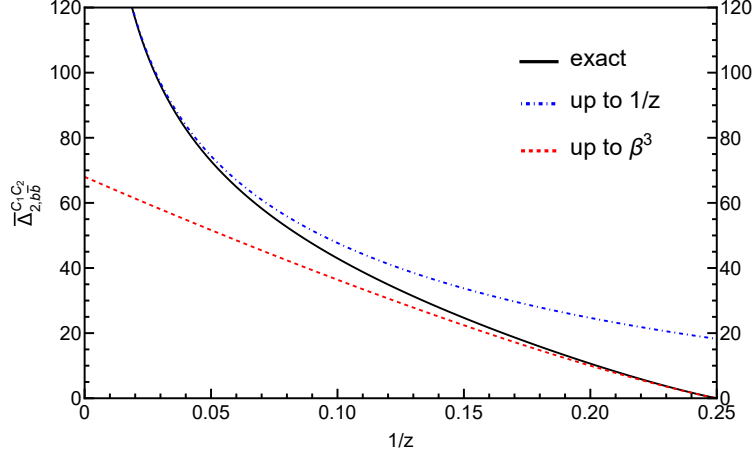


Figure 4: Comparison between the exact result of $\overline{\Delta}_{2,bb}^{C_1 C_2}$ (black line) and its expansion around $z \rightarrow \infty$ (dot-dashed blue line) or $z \rightarrow 1/4$ (dashed red line).

$$\begin{aligned}
& + C_A^2 C_F \beta^3 \left[-\frac{11}{16} \log^2 \left(\frac{\mu^2}{m_H^2} \right) - \frac{11}{12} \log(2) \log \left(\frac{\mu^2}{m_H^2} \right) - \frac{185}{48} \log \left(\frac{\mu^2}{m_H^2} \right) \right. \\
& + \left. \frac{7\zeta(3)}{16} + \frac{5\pi^2 \log(2)}{12} + \frac{5\pi^2}{36} - \frac{11 \log^2(2)}{12} - \frac{61 \log(2)}{72} - \frac{3557}{576} \right] \\
& + C_A C_F^2 \beta^3 \left[-\frac{9}{16} \log^2 \left(\frac{\mu^2}{m_H^2} \right) - \frac{3 \log(2)}{2} \log \left(\frac{\mu^2}{m_H^2} \right) - \frac{15}{16} \log \left(\frac{\mu^2}{m_H^2} \right) \right. \\
& + \left. \frac{13\zeta(3)}{16} - \frac{7\pi^2 \log(2)}{12} + \frac{209\pi^2}{576} - \frac{3 \log^2(2)}{4} - \frac{61 \log(2)}{24} - \frac{37}{64} \right] \\
& + C_A C_F n_l \beta^3 \left[\frac{1}{8} \log^2 \left(\frac{\mu^2}{m_H^2} \right) + \frac{\log(2)}{6} \log \left(\frac{\mu^2}{m_H^2} \right) + \frac{13}{24} \log \left(\frac{\mu^2}{m_H^2} \right) \right. \\
& - \left. \frac{\pi^2}{18} + \frac{\log^2(2)}{6} + \frac{5 \log(2)}{36} + \frac{229}{288} \right] \\
& + C_A C_F \beta^3 \left[\frac{1}{8} \log^2 \left(\frac{\mu^2}{m_H^2} \right) + \frac{\log(2)}{6} \log \left(\frac{\mu^2}{m_H^2} \right) + \frac{13}{24} \log \left(\frac{\mu^2}{m_H^2} \right) \right. \\
& - \left. \frac{37\pi^2}{288} - \frac{\log^2(2)}{6} + \frac{13 \log(2)}{12} + \frac{281}{288} \right] \Big) + \mathcal{O}(\beta^4). \tag{6.14}
\end{aligned}$$

Compared to the LO result in (6.12), it exhibits the same power enhancement as predicted by the Coulomb Green function; see eq. (5.15) of ref. [14].

To illustrate the expansions around the small mass and threshold limits, we show in figure 4 the numerical results of $\overline{\Delta}_{2,bb}^{C_1 C_2}$, which is defined by

$$\overline{\Delta}_{2,bb}^{C_1 C_2} \equiv \Delta_{2,bb}^{C_1 C_2} / \left(\frac{m_H m_b \overline{m}_b(\mu)}{\pi v^2} \right). \tag{6.15}$$

Here we have divided $\Delta_{2,bb}^{C_1 C_2}$ by its overall coupling to expose the dependence of the rest part on z more clearly. The small mass expansion coincides with the exact result for $1/z < 0.05$, while the threshold expansion overlaps with the exact result when $1/z > 0.2$.

7 Numerical result

To give the numerical result of the decay width of $H \rightarrow b\bar{b}$, we take the input parameters

$$\begin{aligned} \overline{m_b}(\overline{m_b}) &= 4.18 \text{ GeV}, & m_b &= 5.07 \text{ GeV}, & m_H &= 125.09 \text{ GeV}, \\ m_t &= 172.69 \text{ GeV}, & \alpha_s(m_Z) &= 0.1181, & G_F &= 1.166378 \times 10^{-5} \text{ GeV}^{-2}, \end{aligned} \quad (7.1)$$

where the on-shell value of m_b is obtained from $\overline{m_b}(\overline{m_b})$ in the $\overline{\text{MS}}$ scheme via the four-loop mass relation [74–77]. The package RunDec [78, 79] was used to obtain $\overline{m_b}$ at other scales, e.g., $\overline{m_b}(m_H/2) = 2.95631 \text{ GeV}$, $\overline{m_b}(m_H) = 2.78425 \text{ GeV}$ and $\overline{m_b}(2m_H) = 2.63908 \text{ GeV}$. The strong coupling at several typical scales is evaluated to be $\alpha_s(m_H/2) = 0.125257$, $\alpha_s(m_H) = 0.112715$ and $\alpha_s(2m_H) = 0.102501$.

In table 1, we show the QCD corrections induced by different combinations of operators. The LO and NLO results are obtained only by considering the Yukawa coupling, exhibiting a NLO correction of 20%. The NNLO correction increases the NLO decay width further by 4%, and begins to receive contributions from the Higgs-gluon-gluon vertices, which account for one third of the $\mathcal{O}(\alpha_s^2)$ correction. The N³LO correction gives rise to 1% improvement with respect to the NNLO result, much larger than the estimated contribution, about 0.2%, from missing higher-order corrections based on the calculation with massless bottom quarks [80]. It is interesting to observe the large higher-order correction in the interference contribution $\Gamma_{Hb\bar{b}}^{C_1C_2}$, about 55%. This is due to the large logarithms $\ln(m_H^2/m_b^2)$ as shown in the analytic result in eq. (6.8).

	[MeV]	$\mu = \frac{1}{2}m_H$	$\mu = m_H$	$\mu = 2m_H$
$\mathcal{O}(\alpha_s^0)$	$\Gamma_{Hb\bar{b}}^{C_2C_2}$	2.1314	1.8905	1.6985
$\mathcal{O}(\alpha_s^1)$	$\Gamma_{Hb\bar{b}}^{C_2C_2}$	0.25813	0.39409	0.47563
$\mathcal{O}(\alpha_s^2)$	$\Gamma_{Hb\bar{b}}^{C_2C_2}$	-0.0043084	0.076819	0.143670
	$\Gamma_{Hb\bar{b}}^{C_1C_2}$	0.027078	0.024746	0.022608
$\mathcal{O}(\alpha_s^3)$	$\Gamma_{Hb\bar{b}}^{C_2C_2}$	-0.015360	0.0048336	0.038198
	$\Gamma_{Hb\bar{b}}^{C_1C_2}$	0.010314	0.013585	0.015170
	$\Gamma_{Hb\bar{b}}^{C_1C_1}$	0.0088676	0.0064617	0.0048595

Table 1: $\Gamma_{Hb\bar{b}}^{C_2C_2}$, $\Gamma_{Hb\bar{b}}^{C_1C_2}$ and $\Gamma_{Hb\bar{b}}^{C_1C_1}$ at different orders of α_s in the mixed mass scheme.

The above results are obtained in the mixed mass scheme, i.e., the Yukawa coupling and the masses in propagators are renormalized in the $\overline{\text{MS}}$ and on-shell schemes, respectively. This scheme is convenient in organizing the calculation. For phenomenological study, it is more relevant to use a unified scheme. Given our analytical results, it is straight forward to derive the result in either the $\overline{\text{MS}}$ or the on-shell scheme. We show the corresponding numerical results of different higher-order corrections in table 2. The results in the $\overline{\text{MS}}$ scheme are very similar to those in the mixed scheme. The two schemes differ in the

renormalization scheme of the mass in propagators. This would affect only the subleading power contribution in the result of $\Gamma_{Hb\bar{b}}^{C_2C_2}$ up to $\mathcal{O}(\alpha_s^2)$, which is highly suppressed by m_b^2/m_H^2 . At $\mathcal{O}(\alpha_s^3)$, the difference arises at leading power, but is still small. The change in the result of $\Gamma_{Hb\bar{b}}^{C_1C_2}$ is obvious because it is proportional to the propagator mass; see eq. (6.2). However, the induced change in the total decay width is not significant due to the suppression of α_s^2 . The scale uncertainty in the $\overline{\text{MS}}$ scheme is 3% and 1% at NNLO and N³LO, respectively. We provide the result of the decay width at N³LO,

$$\Gamma_{H\rightarrow b\bar{b}}^{\text{N}^3\text{LO QCD}}(\overline{\text{MS}}) = 2.410_{-0.017}^{+0.007} \text{ MeV}. \quad (7.2)$$

This accuracy reaches the same level of the experimental expectation. The corrections from finite top quark mass effects are only about 0.001 MeV [15, 73] and thus can be neglected. Including the NLO EW corrections [28], we obtain

$$\Gamma_{H\rightarrow b\bar{b}}^{\text{N}^3\text{LO QCD+NLO EW}}(\overline{\text{MS}}) = 2.382_{-0.017}^{+0.007} \text{ MeV}. \quad (7.3)$$

The results in the on-shell scheme exhibit large higher-order corrections. The LO result is 3.3 (which is just about $m_b^2/\overline{m}_b^2(m_H)$) times of the one in the $\overline{\text{MS}}$ scheme. The decay width is decreased by -35% after including the NLO correction. The NNLO correction reduces the decay width further by -22% . There is still a correction of -10% at N³LO. This poor convergence is caused by the fact that the on-shell mass, as a long-distance definition, suffers from infra-red renormalons [81].

The comparison between the results in the two schemes is shown in figure 5. As more high-order corrections are included, the scale uncertainties become notably smaller, and the difference between the two renormalization schemes is also reduced.

	[MeV]	$\mu = \frac{1}{2}m_H$	$\mu = m_H$	$\mu = 2m_H$
$\Gamma_{H\rightarrow b\bar{b}}(\overline{\text{MS}})$	$\mathcal{O}(\alpha_s^0)$	2.1454	1.9036	1.7108
	$\mathcal{O}(\alpha_s^1)$	0.24806	0.38682	0.47051
	$\mathcal{O}(\alpha_s^2)$	0.014742	0.091773	0.15580
	$\mathcal{O}(\alpha_s^3)$	0.0092203	0.028117	0.055816
$\Gamma_{H\rightarrow b\bar{b}}(\text{OS})$	$\mathcal{O}(\alpha_s^0)$	6.2687	6.2687	6.2687
	$\mathcal{O}(\alpha_s^1)$	-2.4192	-2.1770	-1.9797
	$\mathcal{O}(\alpha_s^2)$	-0.85590	-0.90061	-0.91641
	$\mathcal{O}(\alpha_s^3)$	-0.23550	-0.33107	-0.39831

Table 2: The result of the decay width in the $\overline{\text{MS}}$ or the on-shell schemes.

8 Conclusion

We have calculated the analytic result of the dominant decay channel of the Higgs boson, $H \rightarrow b\bar{b}$, at $\mathcal{O}(\alpha_s^3)$. For the process induced by the bottom quark Yukawa coupling y_b , we

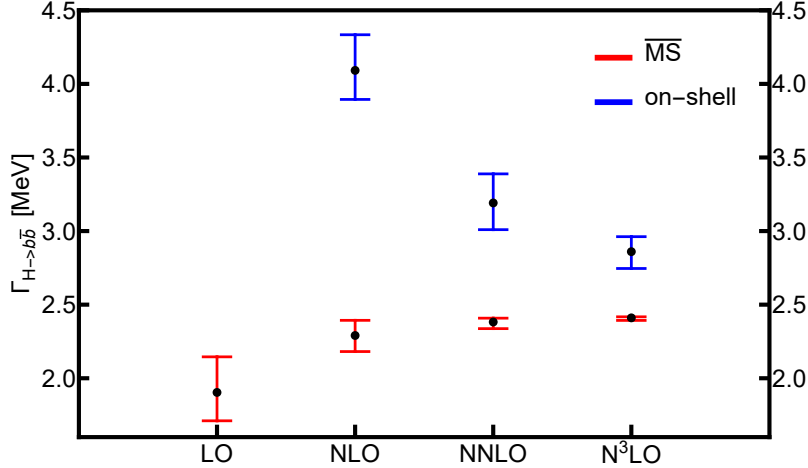


Figure 5: Comparison of the results in the $\overline{\text{MS}}$ and the on-shell schemes. The error bars denote the scale uncertainties.

retain full bottom quark mass dependence up to NNLO but use the result with massless final-state bottom quarks for the $\mathcal{O}(\alpha_s^3)$ correction. The higher-power mass effects in this process are tiny due to the small Taylor expansion parameter m_b^2/m_H^2 . For the process induced by the top quark Yukawa coupling y_t , we perform the calculation always with finite m_b . We consider the contributions from both two and four massive bottom quarks in the final states. The result of the former can be expressed in terms of multiple polylogarithms, while the latter needs elliptic integrals. The asymptotic expansion of the decay width for $H \rightarrow b\bar{b}$ in the small m_b limit shows double logarithmic enhancement from $\mathcal{O}(\alpha_s^2)$. The coefficient of the double logarithm at $\mathcal{O}(\alpha_s^3)$ is proportional to $C_A - C_F$, which is a typical color structure in the subleading power resummation with soft quarks. Our analytic results can be used to check the resummation formula in future. The $\mathcal{O}(\alpha_s^3)$ correction increases the NNLO decay rate by 1%, much larger than expectation from naive power counting of α_s . This improvement is mainly due to the large logarithms as mentioned above. Combining our result with the NLO EW corrections, we provide the most accurate prediction for the $H \rightarrow b\bar{b}$ decay with a scale uncertainty of 1% in the $\overline{\text{MS}}$ scheme of the bottom quark mass renormalization. The results in the on-shell scheme exhibit poor convergence. However, the difference between the two schemes reduces as more higher-order corrections are included.

Acknowledgements

We thank Lorenzo Tancredi for discussions. This work was supported in part by the National Science Foundation of China (grant Nos. 12405117, 12005117, 12321005, 12375076), the Taishan Scholar Foundation of Shandong province (tsqn201909011) and the Deutsche Forschungsgemeinschaft (DFG, German Research Foundation) under Germany’s Excellence Strategy – EXC-2094 – 390783311. J. W. and X. W. thank the Munich Institute for Astro-, Particle and BioPhysics (MIAPbP), which is funded by the same DFG grant, for hospitality during part of the work.

A Topologies of the master integrals

The topology diagrams of the master integrals in the NP1 and P1 families are displayed in figure 6 and figure 7, respectively.

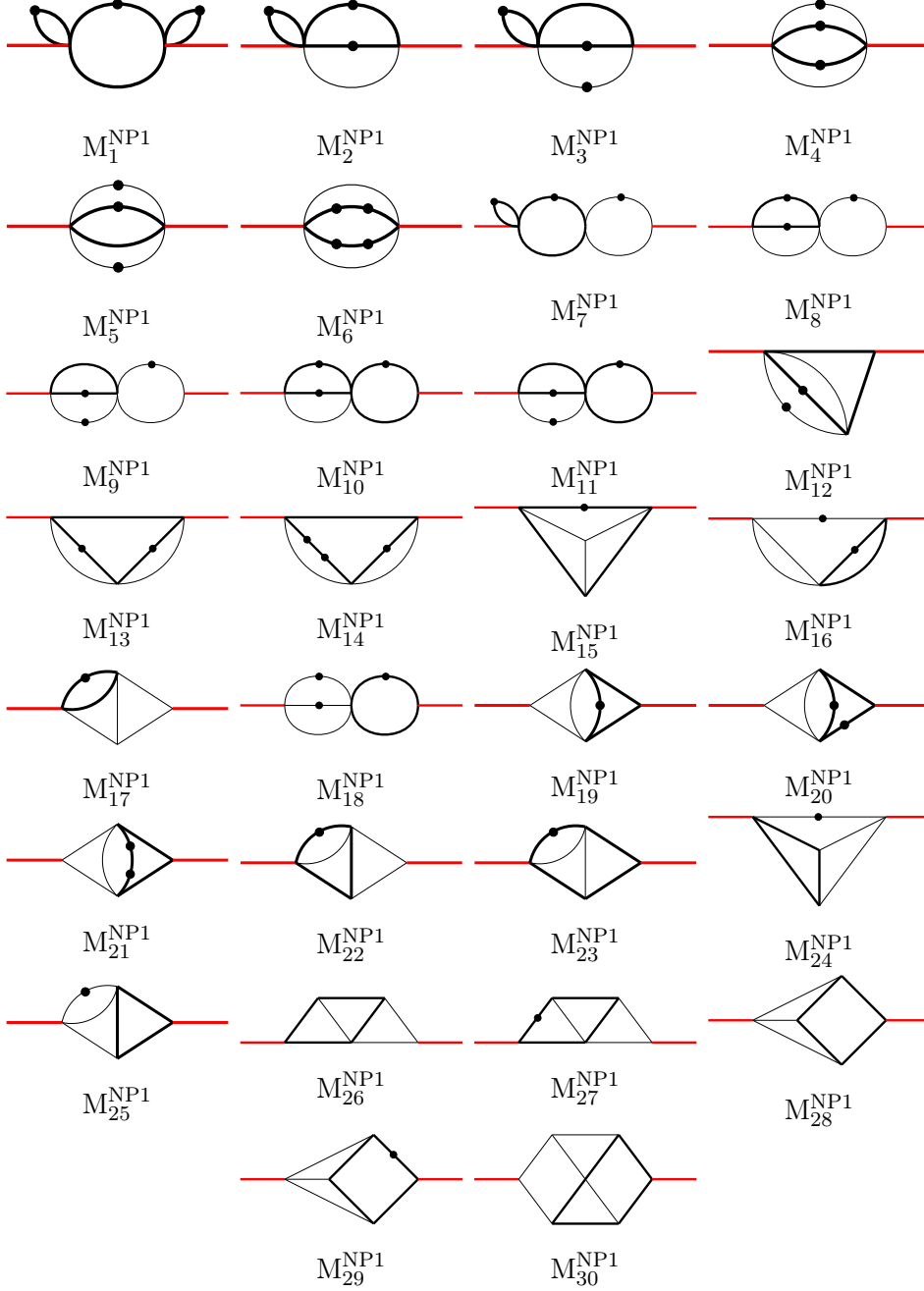


Figure 6: Master integrals in the NP1 topology. The thick black and red lines stand for the massive bottom quark and the Higgs boson, respectively. One black dot indicates one additional power of the corresponding propagator.

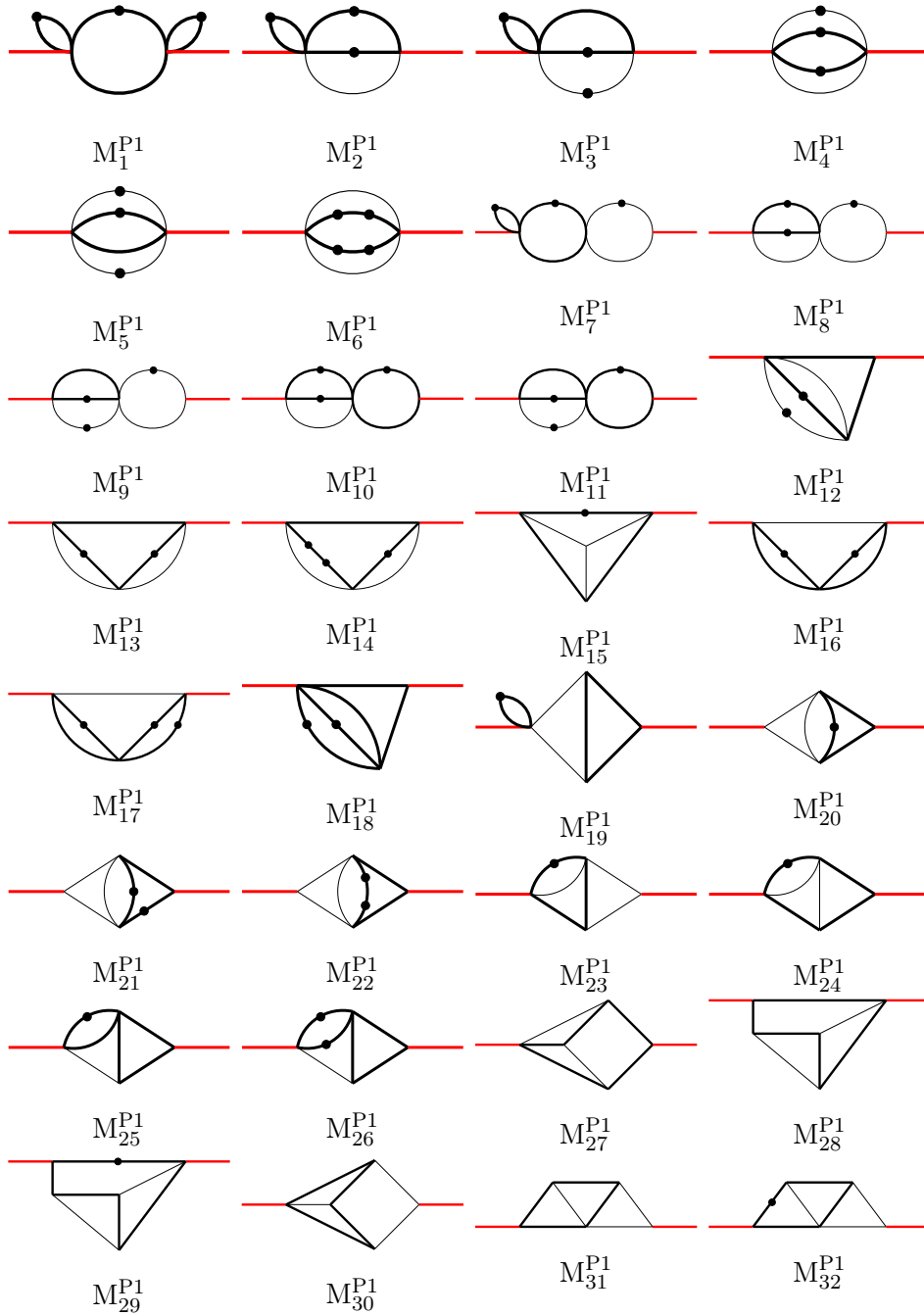


Figure 7: Master integrals in the P1 topology. The thick black and red lines stand for the massive bottom quark and the Higgs boson, respectively. One black dot indicates one additional power of the corresponding propagator.

B The canonical form of the three-loop kite integral family

As mentioned in section 3, the master integral M_{30}^{P1} , dubbed the three-loop kite integral, in the P1 topology does *not* contribute to the decay rate at $\mathcal{O}(\alpha_s^3)$. However, it may contribute

at higher orders. In addition, the calculation of this integral and its sub-sectors is highly non-trivial and representative for multi-loop Feynman integrals. Specifically, it has the three-loop equal-mass banana integral family as its sub-sector. The geometry rooted in this three-loop banana integral family is a K3 surface, which is related to the symmetric product of the elliptic curve corresponding to the sunrise integral (two-loop equal-mass banana integral). The higher sectors of the three-loop kite family have 7 master integrals and the related geometry is a Riemann sphere⁵. As a proof of concept, we derive the ϵ -factorized differential equation for both the elliptic (or beyond elliptic) sub-sectors and higher sectors in this family. Our method is general and can be extended to other (two-scale) problems. Similar geometric structures have been discovered in the two-loop kite integral [82–84], in which only one master integral is present in the higher sector than the sunrise integrals. Recently, the three-loop corrections to the electron self-energy have been calculated in [85], where the elliptic curve related to the sunrise integral plays an important role. However, there is no support for a cut on four massive particles and thus the three-loop banana integral does not appear as a sub-sector⁶.

The three-loop kite family possesses 10 master integrals. The first three constitute the three-loop banana family⁷. The remaining 7 master integrals are in higher sectors. The structure of the differential equation for a pre-canonical basis reads

$$\frac{d}{dz} \begin{pmatrix} \vec{I}_{\text{banana}} \\ \vec{I}_{\text{higher}} \end{pmatrix} = \begin{pmatrix} \mathbf{D}_{3 \times 3}^{\text{banana}}(\epsilon, z) & \mathbf{0}_{3 \times 7} \\ \mathbf{N}_{7 \times 3}^{\text{banana}}(\epsilon, z) & \mathbf{D}_{7 \times 7}^{\text{higher}}(\epsilon, z) \end{pmatrix} \begin{pmatrix} \vec{I}_{\text{banana}} \\ \vec{I}_{\text{higher}} \end{pmatrix}, \quad (\text{B.1})$$

where we highlight the non-vanishing blocks in colors. We first bring the diagonal blocks into ϵ -form from lower to higher sectors, and then deal with non-diagonal blocks. We adopt the results in [86] to bring the 3×3 diagonal block for the banana integrals to the canonical form. Then we focus on the 7×7 diagonal block, which involves the top integral, M_{30}^{P1} . This is the most interesting part, and we will elaborate our method in detail, which can be useful for other Feynman integrals. In the end, we turn to the non-diagonal part, which describes the mixing with the banana family.

Feynman integrals are characterized by their corresponding geometries, which can be detected from the maximal cuts (or the variety of graph polynomials). A Riemann sphere corresponds to the functional space of MPLs. An elliptic curve (torus) leads to the functional space of elliptic MPLs (eMPLs) and modular forms. Higher-dimensional generalizations like Calabi-Yau n -folds or higher-genus generalizations like hyperelliptic curves indicate more complicated functional spaces. Readers are referred to [87, 88] for reviews, and to [85, 89, 90] and references therein for recent examples.

In our case, the three-loop banana sub-sector features a Calabi-Yau 2-folds, also called a K3 surface, while the higher sectors are related to a Riemann sphere except for the dependence on the banana sub-sector through mixing. We propose an efficient and systematic

⁵The K3 geometry enters only through the sub-sector dependence from the banana sector.

⁶Such a cut on four massive particles exists in the three-loop QED corrections to the photon propagator. There is a similar topology to the three-loop kite integral in our case. We thank Lorenzo Tancredi for pointing out this.

⁷Since we impose a four- b cut, the tadpole does not contribute. We hence suppress it from the start.

way to find the ϵ -factorized differential equation of the three-loop kite family, i.e., we apply the method developed to calculate the equal-mass banana integrals [86, 91, 92] to the integrals characterized by a Riemann sphere⁸ so that we can also use “periods” to construct the desired basis in higher sectors. In this unified language, we are able to give a criterion to choose a good pre-canonical basis and to explain the required rationalization in terms of the generalized “mirror map” in higher sectors.

In the following, we briefly review existing results in the banana sub-sectors and then dive into the higher sectors. After that we deal with their mixing with the banana family. We give the ϵ -factorized differential equation for the entire family at the end.

B.1 Banana sector

The relevant pre-canonical master integrals in this sector are simply $I_{011100100}^{\text{P1}}$, $I_{021100100}^{\text{P1}}$ and $I_{031100100}^{\text{P1}}$. The banana integrals are naturally set around the spacetime dimension $D = 2$, which is related to the results around $D = 4$ by the dimension-shift operator \mathbf{D}^- , which lowers the dimension of spacetime by two through

$$\mathbf{D}^- I_{\nu_1\nu_2\nu_3\nu_4\nu_5\nu_6\nu_7\nu_8\nu_9}^{\text{P1}}(D) = I_{\nu_1\nu_2\nu_3\nu_4\nu_5\nu_6\nu_7\nu_8\nu_9}^{\text{P1}}(D-2). \quad (\text{B.2})$$

Then the canonical basis is given by [91]

$$\begin{aligned} F_1 &= \frac{\mathbf{D}^- I_{011100100}^{\text{P1}}(4-2\epsilon, z)}{\psi_1(z)}, \\ F_2 &= \frac{1}{\epsilon} \frac{1}{2\pi i} \frac{d}{d\tau} F_1 + \left[G_2(z) + \frac{2(z-10)}{(z-4)(z-16)W(z)} \psi_1(z) \right] F_1, \\ F_3 &= \frac{1}{\epsilon} \frac{1}{2\pi i} \frac{d}{d\tau} F_2 + \left[-2G_2(z) + \frac{2(z-10)}{(z-4)(z-16)W(z)} \psi_1(z) \right] F_2, \\ &\quad + \left[\frac{3}{2} G_2^2(z) - \frac{(z+8)^2(z^2-8z+64)}{2z^2(z-4)^2(z-16)^2 W^2(z)} \psi_1^2(z) \right] F_1, \end{aligned} \quad (\text{B.3})$$

with the mirror map

$$\tau = \frac{\psi_2(z)}{\psi_1(z)}, \quad q = e^{2\pi i \tau}, \quad (\text{B.4})$$

where ψ_1 and ψ_2 are periods of the K3 surface⁹ and are annihilated by the corresponding Picard-Fuchs operators. The Wronskian $W(z)$ reads

$$W(z) = \frac{-12}{z \sqrt{(z-4)(z-16)}}. \quad (\text{B.5})$$

The inverse relation between τ and z is [93]

$$z = - \left(\frac{\eta(\tau)\eta(3\tau)}{\eta(2\tau)\eta(6\tau)} \right)^6, \quad (\text{B.6})$$

⁸In the sense that the involved geometry is simpler, our method is a degeneration.

⁹It turns out that $\psi_1 \propto \phi_1^2$ and $\psi_2 \propto \phi_1\phi_2$, where ϕ_1 and ϕ_2 are the two periods of an elliptic curve. In this sense, the K3 surface is called a symmetric product of the corresponding elliptic curve.

where $\eta(\tau)$ is the Dedekind eta function. The Jacobian from z to the modular variable τ reads

$$J(z) = \frac{1}{2\pi i} \frac{dz}{d\tau} = \frac{\psi_1(z)}{W(z)}. \quad (\text{B.7})$$

The coefficient function $G_2(z)$ reads

$$G_2(z) = (2\pi i)^2 \int_{i\infty}^{\tau} d\tau_1 \int_{i\infty}^{\tau_1} d\tau_2 \frac{\tilde{z}(\tilde{z}-8)(\tilde{z}+8)^3}{864(4-\tilde{z})^{\frac{3}{2}}(16-\tilde{z})^{\frac{3}{2}}} \psi_1^6(\tilde{z}), \quad (\text{B.8})$$

where the integrand is viewed as a function of τ_2 through $\tilde{z}(\tau_2)$ given by (B.6). Then the canonical differential equation reads

$$\frac{1}{2\pi i} \frac{d}{d\tau} \begin{pmatrix} F_1 \\ F_2 \\ F_3 \end{pmatrix} = \epsilon \begin{pmatrix} -f_{2,a} - f_{2,b} & 1 & 0 \\ f_{4,b} & -f_{2,a} + 2f_{2,b} & 1 \\ f_6 & f_{4,b} & -f_{2,a} - f_{2,b} \end{pmatrix} \begin{pmatrix} F_1 \\ F_2 \\ F_3 \end{pmatrix} \quad (\text{B.9})$$

with the above matrix elements being (meromorphic and/or quasi-Eichler) modular forms. Their explicit expressions, which can be found in [91], are not relevant for this work. In practice, one does not need to calculate (B.8) and the above matrix elements in a closed form. But rather, one can perform expansion in q via the mirror map. The evaluation of the iterated integrals in terms of q is extremely fast.

B.2 Higher sectors

Now we turn to the interesting part in this section, i.e., the higher sectors. Apart from the K3 geometry inherited from the sub-sector, it also has a (punctured) Riemann sphere inside, which is related to the function space of MPLs. It turns out that we can use the same method as in the banana family, i.e., constructing an ansatz using periods and the mirror map to change the variable, in order to derive the canonical form. In this context, the rationalization transformation in (3.7) and (3.8) is dictated by the geometry.

The complexity of Feynman integrals usually increases with the number of the propagators. Normally a pre-canonical basis can already transform the differential equation system into a lower block-triangular form. In our case, there are 7 master integrals apart from the three banana integrals after using LiteRed [94]. Since we are working around $D = 4$, it is natural to raise the powers of some propagators. The following 7 pre-canonical master integrals are judiciously chosen:

$$\begin{aligned} M_4 &= \epsilon^3(1-2\epsilon) m_b^2 I_{011201200}^{\text{P1}}(4-2\epsilon, z), \\ M_5 &= \epsilon^4(1-2\epsilon) m_b^2 I_{111101200}^{\text{P1}}(4-2\epsilon, z), \\ M_6 &= \epsilon^3(1-2\epsilon) m_b^4 I_{111201200}^{\text{P1}}(4-2\epsilon, z), \\ M_7 &= \epsilon^5(1-2\epsilon) m_b^2 I_{111111100}^{\text{P1}}(4-2\epsilon, z), \\ M_8 &= \epsilon^4(1-2\epsilon)^2 m_b^2 I_{011111110}^{\text{P1}}(4-2\epsilon, z), \\ M_9 &= \epsilon^4(1-2\epsilon) m_b^4 I_{021111110}^{\text{P1}}(4-2\epsilon, z), \\ M_{10} &= \epsilon^5(1-2\epsilon) m_b^2 I_{111110110}^{\text{P1}}(4-2\epsilon, z). \end{aligned} \quad (\text{B.10})$$

Note that the master integrals M_7, M_8, M_9 are reducible, and belong to the sub-sectors of M_{10} , which is proportional to M_{30}^{P1} . The normalization factors have been fixed such that M_i do not have divergences, which can be easily determined from the differential equation. With this setup, the 7×7 diagonal block in (B.1) in the higher sectors looks like

$$\mathbf{D}_{7 \times 7}^{\text{higher}}(\epsilon, x) = \begin{pmatrix} \mathbf{d}_{1 \times 1}^{(1)} & \mathbf{0}_{1 \times 2} & \mathbf{0}_{1 \times 3} & \mathbf{0}_{1 \times 1} \\ \mathbf{n}_{2 \times 1}^{(1)} & \mathbf{d}_{2 \times 2}^{(2)} & \mathbf{0}_{2 \times 3} & \mathbf{0}_{2 \times 1} \\ \mathbf{n}_{3 \times 1}^{(2)} & \mathbf{n}_{3 \times 2}^{(3)} & \mathbf{d}_{3 \times 3}^{(3)} & \mathbf{0}_{3 \times 1} \\ 0 & \mathbf{n}_{1 \times 2}^{(4)} & \mathbf{n}_{1 \times 3}^{(5)} & \mathbf{d}_{1 \times 1}^{(4)} \end{pmatrix}. \quad (\text{B.11})$$

The strategy is always firstly to bring the upper diagonal blocks (corresponding to a lower sector) into the ϵ -factorized form, and then to deal with the corresponding off-diagonal mixing in the same row¹⁰. After that, we turn to lower blocks (higher sectors) and repeat the procedure until the whole matrix is in the ϵ -factorized form.

The first 1×1 block $\mathbf{d}_{1 \times 1}^{(1)}$ is trivial. The $\mathcal{O}(\epsilon^0)$ part is removed by solving a first-order homogeneous differential equation. This equation is nothing but the simplest Picard-Fuchs equation (a degree-one differential equation) with a solution $\omega_1(z) = \sqrt{(z-4)/z}$. Thus the desired master integral reads

$$F_4 = \frac{M_4}{\omega_1(z)} = \sqrt{\frac{z}{z-4}} M_4. \quad (\text{B.12})$$

We elaborate in detail on the next 2×2 block. The fact that $\mathbf{d}_{2 \times 2}^{(2)}$ is not degenerate indicates $(M_5, dM_5/dz)$ furnishes a basis. Then we can easily derive a second-order differential operator for M_5 as¹¹

$$\left[\overbrace{\frac{d^2}{dz^2} + \frac{3\epsilon z + 3z - 10}{(z-4)z} \frac{d}{dz} + \frac{(1+2\epsilon)(\epsilon z + 2\epsilon + z - 2)}{(z-4)z^2}}^{\hat{L}_{2,(2)}^{(\epsilon)}(z)} \right] M_5 = \text{lower-sector integrals}. \quad (\text{B.13})$$

It suffices to consider the maximal cut in this sector (i.e., taking the involved 6 propagators on-shell) so that the lower-sector integrals on the right-hand side vanish. The operator $\hat{L}_{2,(2)}^{(\epsilon)}(z)$ is the Picard-Fuchs operator for this integral. It turns out that it factorizes linearly when $\epsilon = 0$, which is a typical property for integrals related to MPLs¹²,

$$\hat{L}_{2,(2)}^{(\epsilon=0)}(z) = \left[\frac{d}{dz} + \frac{2(z-3)}{z(z-4)} \right] \left[\frac{d}{dz} + \frac{1}{z} \right]. \quad (\text{B.14})$$

$\hat{L}_{2,(2)}^{(\epsilon=0)}(z)$ has the following two solutions:

$$\omega_{2,1}(z) = \frac{1}{z}, \quad \omega_{2,2}(z) = \frac{1}{2\pi i} \frac{1}{z} \log \frac{2 + \sqrt{z(z-4)} - z}{2}, \quad (\text{B.15})$$

¹⁰This mixing is within the 7×7 block, not the mixing with the banana family.

¹¹Readers are referred to the book [88] for details on the Picard-Fuchs operators in the context of Feynman integrals.

¹²For integrals beyond MPLs, the corresponding Picard-Fuchs operators do not factorize linearly.

where we have chosen a normalization for later convenience. The solutions can be obtained by the method of variation of parameters. The first solution $\omega_{2,1}(z)$ corresponds to the rightmost factorized operator in (B.14) and is holomorphic on the Riemann sphere, especially around the infinite, which is the point of maximal unipotent monodromy (MUM). We will explain in more detail about the MUM point later on. The second solution $\omega_{2,2}(z)$ has logarithmic singularity and is related to the leftmost factorized operator. We call these two solutions “periods”, although the related geometric object is a Riemann sphere, which has no non-trivial 1-cycle to define the period integral¹³. Then we can formally define the “mirror map” by

$$\tau_2 \equiv \frac{\omega_{2,2}(z)}{\omega_{2,1}(z)}, \quad q_2 = e^{2\pi i \tau_2} = \frac{2 + \sqrt{z(z-4)} - z}{2}. \quad (\text{B.16})$$

It is remarkable that the variable q_2 , an analogue of q in the elliptic case, is just the variable w in eq. (3.8), which is introduced to rationalize the square root $\sqrt{z(z-4)}$. This procedure provides a geometric way to find the proper variable transformation for rationalization of square roots that appear in the differential equations.

Now we can write a similar ansatz for the canonical basis in this sector as in the elliptic case:

$$F_5 = \frac{M_5}{\omega_{2,1}(z)}, \quad F_6 = \frac{1}{\epsilon} \frac{1}{2\pi i} \frac{d}{d\tau_2} F_5 - t_{11}(z) F_5, \quad (\text{B.17})$$

where $t_{11}(z)$ is a rotation coefficient depending on z . By requiring the differential equation is in ϵ -factorized form, it is determined to be

$$t_{11}(z) = -\sqrt{\frac{z-4}{z}}. \quad (\text{B.18})$$

The mixing of this 2×2 sector with F_4 is simple and can be cast in ϵ -factorized form by refining F_6 as

$$F_6 = \frac{1}{\epsilon} \frac{1}{2\pi i} \frac{d}{d\tau_2} F_5 - t_{11}(z) F_5 - \frac{3z}{2} F_4. \quad (\text{B.19})$$

The most non-trivial part is the 3×3 block $\mathbf{d}_{3 \times 3}^{(3)}$. The Picard-Fuchs operators for a general 3×3 differential matrix should have degree 3 and will factorize into linear operators when $\epsilon = 0$ if the corresponding solution can be written in terms of MPLs. The Picard-Fuchs operator for M_9 is of degree 3. Setting $\epsilon = 0$, we have

$$\overbrace{\left[\frac{d^3}{dz^3} + \frac{8z-22}{z(z-4)} \frac{d^2}{dz^2} + \frac{14z-22}{z^2(z-4)} \frac{d}{dz} + \frac{4z-2}{z^3(z-4)} \right]}^{\hat{L}_{3,(3)}^{(\epsilon=0)}(z)} M_9 = \text{lower-sector integrals} + \mathcal{O}(\epsilon). \quad (\text{B.20})$$

We find that this operator factorizes into three linear operators. In principle, one uses the information from this operator to construct a basis in this sector. This operator has three regular singularities: $\{0, 4, \infty\}$. Around these regular singularities, one can use the Frobenius method to construct three solutions in terms of series expansions [95]. The

¹³Such “periods” also play an important role in decomposing the connection matrix into semi-simple and unipotent parts in [90], e.g., eq. (3.13) therein.

leading behavior of the three solutions around each point z_i is of the form $(z - z_i)^{\rho_{i,j}}$, where $z_i \in \{0, 4, \infty\}$ and $j = 1, 2, 3$.

When all the indices are equal, $\rho_{i,1} = \rho_{i,2} = \rho_{i,3}$, one of the three solutions is holomorphic around such a point¹⁴, while the second and third solution develops single and double logarithmic structure, respectively. In this context, the logarithmic structure is maximal, and the regular singularity z_i is called a MUM point. The operator with a MUM point is nice, since one can use it to define the desired mirror map. In the case of (B.14), the MUM point is $z = \infty$, around which the two solutions are holomorphic and singly logarithmic, respectively. They are used to formally define the generalized “mirror map” (B.16). If $\hat{L}_{3,(3)}^{(\epsilon=0)}(z)$ processes a MUM point, then there will be one more generalized “period”, which is doubly logarithmic. This period can be used to define an additional so-called Y -invariant [96], which has appeared in the calculation of Calabi-Yau related Feynman integrals, like the banana integrals starting from four loops [86, 92] and the ice-cone integrals [97]. A first application of the Y -invariant in elliptic Feynman integrals can be found in [89]. However, $\hat{L}_{3,(3)}^{(\epsilon=0)}(z)$ does not have a MUM point, as shown by the following table. Hence, we

	$z = 0$	$z = 4$	$z = \infty$
ρ_1	$-1/2$	0	1
ρ_2	-1	1	2
ρ_3	-1	$-1/2$	2

Table 3: The leading behaviors of the three solutions around regular singularities of $\hat{L}_{3,(3)}^{(\epsilon=0)}$.

conclude that it is not a nice operator, and its related Feynman integrals are not a proper pre-canonical basis to start with. We believe that this criterion for choosing a nice operator and canonical basis can be applicable to other cases.

Following the same logic, the Picard-Fuchs operator for M_8 has three singularities: $z = 0, 4$ and ∞ . The first two are regular singularities, but not MUM points and the last one is not even a regular singularity because this operator is in fact a reduced operator of degree-2 for dM_8/dz . Therefore, we do not choose M_8 as a good pre-canonical master integral either.

The Picard-Fuchs operator for M_7 is exactly the same as $\hat{L}_{2,(2)}^{(\epsilon)}(z)$, which has proven to be a nice operator. Here we reuse the previous results and the first two basis integrals can be tentatively chosen,

$$F_7 = \frac{M_7}{\omega_{2,1}(z)}, \quad F_8 = \frac{1}{\epsilon} \frac{1}{2\pi i} \frac{d}{d\tau_2} F_7 - t_{11}(z) F_7, \quad (\text{B.21})$$

following the same form as (B.17). Since $\hat{L}_{2,(2)}^{(\epsilon)}(z)$ is of degree-2, M_7 and its derivatives do not have any dependence on the third basis in this block. The candidates for the third basis include M_8 , dM_8/dz , M_9 . It turns out that M_8 or dM_8/dz are not good, since their ϵ -factorized differential equations are not of Fuchsian form. So we choose M_9 to proceed.

¹⁴Note that $\rho_{i,j}$ may not be an integer, but a rational number. Then holomorphicity is a feature of the series with $(z - z_i)^{\rho_{i,j}}$ stripped off.

Its derivative depends on F_8 at $\mathcal{O}(\epsilon^0)$ and this dependence can be removed by a rotation of the bases. The same trick applies to the mixing of this sector with lower sectors. We obtain the canonical basis as

$$\begin{aligned} F_7 &= \frac{M_7}{\omega_{2,1}(z)}, \\ F_8 &= \frac{1}{\epsilon} \frac{1}{2\pi i} \frac{d}{d\tau_2} F_7 - t_{11}(z)F_7 + t_{11}(z)F_5, \\ F_9 &= zM_9 + \frac{1}{2}t_{11}(z)F_8. \end{aligned} \tag{B.22}$$

At last, we come to the last 1×1 block, which is the top sector integral M_{10} . We get rid of the $\mathcal{O}(\epsilon^0)$ terms in the differential equation of M_{10} by solving a trivial equation, and the differential equation is converted to the canonical form with the definition of the basis

$$F_{10} = zM_{10}. \tag{B.23}$$

So far we have not taken the mixing with the banana sector into account. We turn to this part in the following.

B.3 Mixing

With the above setup, all the mixing of higher sectors to the banana sector has been set in canonical form except for the following two parts,

$$\begin{aligned} \frac{d}{dz} F_4 &= -\frac{(z+2)\psi_1(z)}{12(z-4)\sqrt{z(z-4)}} F_1 + \dots, \\ \frac{d}{dz} F_6 &= -\frac{z(z-22)\psi_1(z) + z(z^2 - 20z + 64)\psi_1'(z)}{24(z-4)\sqrt{z(z-4)}} F_1 + \dots, \end{aligned} \tag{B.24}$$

where the dots denote the ϵ -factorized terms and $\psi_1'(z) = d\psi_1(z)/dz$. Then we can rotate F_4 and F_6 a bit with F_1 to get rid of the above non- ϵ -factorized terms,

$$\begin{aligned} F_4 &= \sqrt{\frac{z}{z-4}} M_4 + G_3(z)F_1, \\ F_6 &= \frac{1}{\epsilon} \frac{1}{2\pi i} \frac{d}{d\tau_2} F_5 - t_{11}(z)F_5 - \frac{3z}{2} F_4 + \left[\frac{\sqrt{z(z-4)}(z-16)\psi_1(z)}{24(z-4)} - 8G_3(z) \right] F_1, \end{aligned} \tag{B.25}$$

with

$$G_3(z) = -2\pi i \int_{i\infty}^{\tau} d\tau_1 \frac{(\tilde{z}+2)\sqrt{\tilde{z}(\tilde{z}-16)}}{144(\tilde{z}-4)} \psi_1^2(\tilde{z}), \tag{B.26}$$

where the integrand is a function of τ_1 via $\tilde{z}(\tau_1)$.

B.4 ϵ -factorized form

We have now obtained the ϵ -factorized differential equation for the three-loop kite family. The result for the banana sector is shown in (B.9), and the result for the higher sectors is

given by

$$\frac{d}{dz} \begin{pmatrix} F_4 \\ \dots \\ F_{10} \end{pmatrix} = \epsilon \mathbf{A}(z) \begin{pmatrix} F_4 \\ \dots \\ F_{10} \end{pmatrix} + \epsilon \mathbf{B}(z) \begin{pmatrix} F_1 \\ F_2 \\ F_3 \end{pmatrix}, \quad (\text{B.27})$$

where

$$\mathbf{A}(z) = \begin{pmatrix} \frac{1}{4-z} & 0 & 0 & 0 & 0 & 0 & 0 \\ \frac{4}{r} & \frac{1}{z} & \frac{1}{2r} & 0 & 0 & 0 & 0 \\ -\frac{24}{z-4} & -\frac{12}{r} & -\frac{4(z-1)}{(z-4)z} & 0 & 0 & 0 & 0 \\ \frac{8(3z-4)}{(z-4)z} & -\frac{12}{r} & 0 & -\frac{4(z-1)}{(z-4)z} & -\frac{12}{r} & 0 & 0 \\ -\frac{8}{r} & 0 & -\frac{1}{2r} & \frac{1}{2r} & \frac{1}{z} & 0 & 0 \\ \frac{4}{r} & -\frac{2}{z} & 0 & -\frac{1}{2r} & -\frac{2}{z} & -\frac{1}{z} & 0 \\ 0 & \frac{2}{z} & 0 & 0 & \frac{2}{z} & 0 & -\frac{1}{z} \end{pmatrix} \quad (\text{B.28})$$

with r defined in (3.7). The non-vanishing matrix elements of \mathbf{B} read

$$\begin{aligned} \mathbf{B}_{41}(z) &= \frac{(z+2)\psi_1(z)}{6\sqrt{z(z-4)^3}} - G_3(z) \left[\frac{1}{z-16} + \frac{G_2(z)}{J(z)} \right], & \mathbf{B}_{42}(z) &= \frac{G_3(z)}{J(z)}, \\ \mathbf{B}_{51}(z) &= -\frac{(z-16)\psi_1(z)}{12(z-4)} + \frac{4G_3(z)}{\sqrt{z(z-4)}}, \\ \mathbf{B}_{61}(z) &= \frac{(z^2-26z+16)\psi_1(z)}{3\sqrt{z(z-4)^3}} + G_3(z) \left[-\frac{8((z-48)z+128)}{(z-16)(z-4)z} + 16\frac{G_2(z)}{J(z)} \right], \\ \mathbf{B}_{62}(z) &= -16\frac{G_3(z)}{J(z)}, \\ \mathbf{B}_{71}(z) &= \frac{(z-16)(5z-4)\psi_1(z)}{12\sqrt{z(z-4)^3}} - \frac{8(3z-4)G_3(z)}{z(z-4)}, \\ \mathbf{B}_{91}(z) &= \frac{(z-16)(3z+4)\psi_1(z)}{48z(z-4)} - \frac{4G_3(z)}{\sqrt{z(z-4)}}. \end{aligned} \quad (\text{B.29})$$

The indices of the matrix \mathbf{B}_{ij} run over $i = 4, \dots, 10$ and $j = 1, 2, 3$. The above matrix elements seem complicated, but they have simple expansions in terms of q . The solutions of the differential equations in terms of Chen-iterated integrals and a comparison with the results obtained in the calculation of three-loop corrections to the photon propagator¹⁵ are left to future work.

References

- [1] ATLAS collaboration, G. Aad et al., *Characterising the Higgs boson with ATLAS data from Run 2 of the LHC*, [2404.05498](#).
- [2] ATLAS collaboration, *Projections for measurements of Higgs boson cross sections, branching ratios, coupling parameters and mass with the ATLAS detector at the HL-LHC*, .
- [3] Y. Zhu, H. Cui and M. Ruan, *The Higgs $\rightarrow b\bar{b}, c\bar{c}$, gg measurement at CEPC*, *JHEP* **11** (2022) 100, [[2203.01469](#)].

¹⁵We thank Lorenzo Tancredi for sharing Felix Forner's thesis [98] in private when we were submitting this manuscript.

- [4] CEPC PHYSICS STUDY GROUP collaboration, H. Cheng et al., *The Physics potential of the CEPC. Prepared for the US Snowmass Community Planning Exercise (Snowmass 2021)*, in *Snowmass 2021*, 5, 2022, [2205.08553](#).
- [5] E. Braaten and J. P. Leveille, *Higgs Boson Decay and the Running Mass*, *Phys. Rev. D* **22** (1980) 715.
- [6] N. Sakai, *Perturbative QCD Corrections to the Hadronic Decay Width of the Higgs Boson*, *Phys. Rev. D* **22** (1980) 2220.
- [7] P. Janot, *First Order QED and QCD Radiative Corrections to Higgs Decay Into Massive Fermions*, *Phys. Lett. B* **223** (1989) 110–118.
- [8] M. Drees and K.-i. Hikasa, *NOTE ON QCD CORRECTIONS TO HADRONIC HIGGS DECAY*, *Phys. Lett. B* **240** (1990) 455.
- [9] A. Dabelstein and W. Hollik, *Electroweak corrections to the fermionic decay width of the standard Higgs boson*, *Z. Phys. C* **53** (1992) 507–516.
- [10] B. A. Kniehl, *Radiative corrections for $H \rightarrow f$ anti- f (γ) in the standard model*, *Nucl. Phys. B* **376** (1992) 3–28.
- [11] W. Bernreuther, L. Chen and Z.-G. Si, *Differential decay rates of CP-even and CP-odd Higgs bosons to top and bottom quarks at NNLO QCD*, *JHEP* **07** (2018) 159, [[1805.06658](#)].
- [12] A. Behring and W. Bizoń, *Higgs decay into massive b-quarks at NNLO QCD in the nested soft-collinear subtraction scheme*, *JHEP* **01** (2020) 189, [[1911.11524](#)].
- [13] G. Somogyi and F. Tramontano, *Fully exclusive heavy quark-antiquark pair production from a colourless initial state at NNLO in QCD*, *JHEP* **11** (2020) 142, [[2007.15015](#)].
- [14] J. Wang, Y. Wang and D.-J. Zhang, *Analytic decay width of the Higgs boson to massive bottom quarks at next-to-next-to-leading order in QCD*, *JHEP* **03** (2024) 068, [[2310.20514](#)].
- [15] K. G. Chetyrkin and A. Kwiatkowski, *Second order QCD corrections to scalar and pseudoscalar Higgs decays into massive bottom quarks*, *Nucl. Phys. B* **461** (1996) 3–18, [[hep-ph/9505358](#)].
- [16] R. Harlander and M. Steinhauser, *Higgs decay to top quarks at $O(\alpha_s^2)$* , *Phys. Rev. D* **56** (1997) 3980–3990, [[hep-ph/9704436](#)].
- [17] A. Primo, G. Sasso, G. Somogyi and F. Tramontano, *Exact Top Yukawa corrections to Higgs boson decay into bottom quarks*, *Phys. Rev. D* **99** (2019) 054013, [[1812.07811](#)].
- [18] S. G. Gorishnii, A. L. Kataev, S. A. Larin and L. R. Surguladze, *Corrected Three Loop QCD Correction to the Correlator of the Quark Scalar Currents and γ (Tot) ($H^0 \rightarrow$ Hadrons)*, *Mod. Phys. Lett. A* **5** (1990) 2703–2712.
- [19] K. G. Chetyrkin, *Correlator of the quark scalar currents and $\Gamma(\text{tot})$ ($H \rightarrow$ hadrons) at $O(\alpha_s^3)$ in pQCD*, *Phys. Lett. B* **390** (1997) 309–317, [[hep-ph/9608318](#)].
- [20] P. A. Baikov, K. G. Chetyrkin and J. H. Kuhn, *Scalar correlator at $O(\alpha_s^4)$, Higgs decay into b-quarks and bounds on the light quark masses*, *Phys. Rev. Lett.* **96** (2006) 012003, [[hep-ph/0511063](#)].
- [21] F. Herzog, B. Ruijl, T. Ueda, J. A. M. Vermaseren and A. Vogt, *On Higgs decays to hadrons and the R-ratio at N^4LO* , *JHEP* **08** (2017) 113, [[1707.01044](#)].
- [22] C. Anastasiou, F. Herzog and A. Lazopoulos, *The fully differential decay rate of a Higgs boson to bottom-quarks at NNLO in QCD*, *JHEP* **03** (2012) 035, [[1110.2368](#)].

- [23] V. Del Duca, C. Duhr, G. Somogyi, F. Tramontano and Z. Trócsányi, *Higgs boson decay into b -quarks at NNLO accuracy*, *JHEP* **04** (2015) 036, [[1501.07226](#)].
- [24] R. Mondini, M. Schiavi and C. Williams, *N^3 LO predictions for the decay of the Higgs boson to bottom quarks*, *JHEP* **06** (2019) 079, [[1904.08960](#)].
- [25] X. Chen, P. Jakubčík, M. Marcoli and G. Stagnitto, *The parton-level structure of Higgs decays to hadrons at N^3 LO*, *JHEP* **06** (2023) 185, [[2304.11180](#)].
- [26] M. S. A. Alam Khan, *Renormalization group summation and analytic continuation from spacelike to timeline regions*, *Phys. Rev. D* **108** (2023) 014028, [[2306.10262](#)].
- [27] A. L. Kataev, *The Order $O(\alpha\alpha_s)$ and $O(\alpha_s^2)$ corrections to the decay width of the neutral Higgs boson to the anti- b b pair*, *JETP Lett.* **66** (1997) 327–330, [[hep-ph/9708292](#)].
- [28] L. Mihaila, B. Schmidt and M. Steinhauser, *$\Gamma(H \rightarrow b\bar{b})$ to order $\alpha\alpha_s$* , *Phys. Lett. B* **751** (2015) 442–447, [[1509.02294](#)].
- [29] W. Bizoń, E. Re and G. Zanderighi, *NNLOPS description of the $H \rightarrow b\bar{b}$ decay with MiNLO*, *JHEP* **06** (2020) 006, [[1912.09982](#)].
- [30] Y. Hu, C. Sun, X.-M. Shen and J. Gao, *Hadronic decays of Higgs boson at NNLO matched with parton shower*, *JHEP* **08** (2021) 122, [[2101.08916](#)].
- [31] R. Mondini and C. Williams, *$H \rightarrow b\bar{b}j$ at next-to-next-to-leading order accuracy*, *JHEP* **06** (2019) 120, [[1904.08961](#)].
- [32] J. Gao, *Higgs boson decay into four bottom quarks in the SM and beyond*, *JHEP* **08** (2019) 174, [[1905.04865](#)].
- [33] R. Mondini, U. Schubert and C. Williams, *Top-induced contributions to $H \rightarrow b\bar{b}$ and $H \rightarrow c\bar{c}$ at $\mathcal{O}(\alpha_s^3)$* , *JHEP* **12** (2020) 058, [[2006.03563](#)].
- [34] K. G. Chetyrkin and M. Steinhauser, *Complete QCD corrections of order $O(\alpha_s^3)$ to the hadronic Higgs decay*, *Phys. Lett. B* **408** (1997) 320–324, [[hep-ph/9706462](#)].
- [35] J. Davies, M. Steinhauser and D. Wellmann, *Completing the hadronic Higgs boson decay at order α_s^4* , *Nucl. Phys. B* **920** (2017) 20–31, [[1703.02988](#)].
- [36] T. Inami, T. Kubota and Y. Okada, *Effective Gauge Theory and the Effect of Heavy Quarks in Higgs Boson Decays*, *Z. Phys. C* **18** (1983) 69–80.
- [37] K. G. Chetyrkin, B. A. Kniehl and M. Steinhauser, *Virtual top quark effects on the $H \rightarrow b$ anti- b decay at next-to-leading order in QCD*, *Phys. Rev. Lett.* **78** (1997) 594–597, [[hep-ph/9610456](#)].
- [38] K. G. Chetyrkin, B. A. Kniehl and M. Steinhauser, *Three loop $O(\alpha_s^2 G(F) M(t)^2)$ corrections to hadronic Higgs decays*, *Nucl. Phys. B* **490** (1997) 19–39, [[hep-ph/9701277](#)].
- [39] K. G. Chetyrkin, B. A. Kniehl and M. Steinhauser, *Decoupling relations to $O(\alpha_s^3)$ and their connection to low-energy theorems*, *Nucl. Phys. B* **510** (1998) 61–87, [[hep-ph/9708255](#)].
- [40] T. Liu and M. Steinhauser, *Decoupling of heavy quarks at four loops and effective Higgs-fermion coupling*, *Phys. Lett. B* **746** (2015) 330–334, [[1502.04719](#)].
- [41] T. Hahn, *Generating Feynman diagrams and amplitudes with FeynArts 3*, *Comput. Phys. Commun.* **140** (2001) 418–431, [[hep-ph/0012260](#)].

- [42] A. Alloul, N. D. Christensen, C. Degrande, C. Duhr and B. Fuks, *FeynRules 2.0 - A complete toolbox for tree-level phenomenology*, *Comput. Phys. Commun.* **185** (2014) 2250–2300, [[1310.1921](#)].
- [43] V. Shtabovenko, R. Mertig and F. Orellana, *FeynCalc 9.3: New features and improvements*, *Comput. Phys. Commun.* **256** (2020) 107478, [[2001.04407](#)].
- [44] V. Shtabovenko, R. Mertig and F. Orellana, *FeynCalc 10: Do multiloop integrals dream of computer codes?*, *Comput. Phys. Commun.* **306** (2025) 109357, [[2312.14089](#)].
- [45] F. V. Tkachov, *A Theorem on Analytical Calculability of Four Loop Renormalization Group Functions*, *Phys. Lett. B* **100** (1981) 65–68.
- [46] K. G. Chetyrkin and F. V. Tkachov, *Integration by Parts: The Algorithm to Calculate beta Functions in 4 Loops*, *Nucl. Phys. B* **192** (1981) 159–204.
- [47] J. Klappert, F. Lange, P. Maierhöfer and J. Usovitsch, *Integral reduction with Kira 2.0 and finite field methods*, *Comput. Phys. Commun.* **266** (2021) 108024, [[2008.06494](#)].
- [48] R. N. Lee and A. I. Onishchenko, *ϵ -regular basis for non-polylogarithmic multiloop integrals and total cross section of the process $e^+e^- \rightarrow 2(Q\bar{Q})$* , *JHEP* **12** (2019) 084, [[1909.07710](#)].
- [49] A. V. Kotikov, *Differential equation method: The Calculation of N point Feynman diagrams*, *Phys. Lett. B* **267** (1991) 123–127.
- [50] J. M. Henn, *Multiloop integrals in dimensional regularization made simple*, *Phys. Rev. Lett.* **110** (2013) 251601, [[1304.1806](#)].
- [51] A. B. Goncharov, *Multiple polylogarithms, cyclotomy and modular complexes*, *Math. Res. Lett.* **5** (1998) 497–516, [[1105.2076](#)].
- [52] L.-B. Chen, J. Wang and Y. Wang, *Analytic NNLO QCD corrections to top quark pair production in electron-positron collisions*, *JHEP* **09** (2024) 014, [[2405.18912](#)].
- [53] C. Duhr and F. Dulat, *PolyLogTools — polylogs for the masses*, *JHEP* **08** (2019) 135, [[1904.07279](#)].
- [54] C. W. Bauer, A. Frink and R. Kreckel, *Introduction to the GiNaC framework for symbolic computation within the C++ programming language*, *J. Symb. Comput.* **33** (2002) 1–12, [[cs/0004015](#)].
- [55] X. Liu, Y.-Q. Ma and C.-Y. Wang, *A Systematic and Efficient Method to Compute Multi-loop Master Integrals*, *Phys. Lett. B* **779** (2018) 353–357, [[1711.09572](#)].
- [56] X. Liu, Y.-Q. Ma, W. Tao and P. Zhang, *Calculation of Feynman loop integration and phase-space integration via auxiliary mass flow*, *Chin. Phys. C* **45** (2021) 013115, [[2009.07987](#)].
- [57] X. Liu and Y.-Q. Ma, *AMFlow: A Mathematica package for Feynman integrals computation via auxiliary mass flow*, *Comput. Phys. Commun.* **283** (2023) 108565, [[2201.11669](#)].
- [58] Z.-F. Liu and Y.-Q. Ma, *Determining Feynman Integrals with Only Input from Linear Algebra*, *Phys. Rev. Lett.* **129** (2022) 222001, [[2201.11637](#)].
- [59] H. Ferguson, D. Bailey and S. Arno, *Analysis of PSLQ, an integer relation finding algorithm*, *Math. Comp.* **68** (1999) 351.
- [60] W. E. Caswell, *Asymptotic Behavior of Nonabelian Gauge Theories to Two Loop Order*, *Phys. Rev. Lett.* **33** (1974) 244.

- [61] D. R. T. Jones, *Two Loop Diagrams in Yang-Mills Theory*, *Nucl. Phys. B* **75** (1974) 531.
- [62] M. Czakon, A. Mitov and S. Moch, *Heavy-quark production in gluon fusion at two loops in QCD*, *Nucl. Phys. B* **798** (2008) 210–250, [[0707.4139](#)].
- [63] K. Melnikov and T. v. Ritbergen, *The Three loop relation between the \overline{MS} -bar and the pole quark masses*, *Phys. Lett. B* **482** (2000) 99–108, [[hep-ph/9912391](#)].
- [64] M. I. Kotsky and O. I. Yakovlev, *On the resummation of double logarithms in the process $Higgs \rightarrow \gamma\gamma$* , *Phys. Lett. B* **418** (1998) 335–344, [[hep-ph/9708485](#)].
- [65] T. Liu and A. A. Penin, *High-Energy Limit of QCD beyond the Sudakov Approximation*, *Phys. Rev. Lett.* **119** (2017) 262001, [[1709.01092](#)].
- [66] Z. L. Liu and M. Neubert, *Factorization at subleading power and endpoint-divergent convolutions in $h \rightarrow \gamma\gamma$ decay*, *JHEP* **04** (2020) 033, [[1912.08818](#)].
- [67] J. Wang, *Resummation of double logarithms in loop-induced processes with effective field theory*, [[1912.09920](#)].
- [68] A. Vogt, *Leading logarithmic large- x resummation of off-diagonal splitting functions and coefficient functions*, *Phys. Lett. B* **691** (2010) 77–81, [[1005.1606](#)].
- [69] Z. L. Liu, M. Neubert, M. Schnubel and X. Wang, *Factorization at next-to-leading power and endpoint divergences in $gg \rightarrow h$ production*, *JHEP* **06** (2023) 183, [[2212.10447](#)].
- [70] I. Moulst, I. W. Stewart, G. Vita and H. X. Zhu, *The Soft Quark Sudakov*, *JHEP* **05** (2020) 089, [[1910.14038](#)].
- [71] M. Beneke, M. Garny, S. Jaskiewicz, R. Szafron, L. Vernazza and J. Wang, *Large- x resummation of off-diagonal deep-inelastic parton scattering from d -dimensional refactorization*, *JHEP* **10** (2020) 196, [[2008.04943](#)].
- [72] M. Beneke, M. Garny, S. Jaskiewicz, J. Strohm, R. Szafron, L. Vernazza et al., *Next-to-leading power endpoint factorization and resummation for off-diagonal “gluon” thrust*, *JHEP* **07** (2022) 144, [[2205.04479](#)].
- [73] S. A. Larin, T. van Ritbergen and J. A. M. Vermaseren, *The Large top quark mass expansion for Higgs boson decays into bottom quarks and into gluons*, *Phys. Lett. B* **362** (1995) 134–140, [[hep-ph/9506465](#)].
- [74] D. J. Broadhurst, N. Gray and K. Schilcher, *Gauge invariant on-shell $Z(2)$ in QED, QCD and the effective field theory of a static quark*, *Z. Phys. C* **52** (1991) 111–122.
- [75] N. Gray, D. J. Broadhurst, W. Grafe and K. Schilcher, *Three Loop Relation of Quark (Modified) M_s and Pole Masses*, *Z. Phys. C* **48** (1990) 673–680.
- [76] P. Marquard, A. V. Smirnov, V. A. Smirnov and M. Steinhauser, *Quark Mass Relations to Four-Loop Order in Perturbative QCD*, *Phys. Rev. Lett.* **114** (2015) 142002, [[1502.01030](#)].
- [77] P. Marquard, A. V. Smirnov, V. A. Smirnov, M. Steinhauser and D. Wellmann, *\overline{MS} -on-shell quark mass relation up to four loops in QCD and a general $SU(N)$ gauge group*, *Phys. Rev. D* **94** (2016) 074025, [[1606.06754](#)].
- [78] K. G. Chetyrkin, J. H. Kuhn and M. Steinhauser, *RunDec: A Mathematica package for running and decoupling of the strong coupling and quark masses*, *Comput. Phys. Commun.* **133** (2000) 43–65, [[hep-ph/0004189](#)].
- [79] F. Herren and M. Steinhauser, *Version 3 of RunDec and CRunDec*, *Comput. Phys. Commun.* **224** (2018) 333–345, [[1703.03751](#)].

- [80] M. Spira, *Higgs Boson Decays: Theoretical Status*, *CERN Yellow Reports: Monographs* **3** (2020) 123–134.
- [81] M. Beneke, *Renormalons*, *Phys. Rept.* **317** (1999) 1–142, [[hep-ph/9807443](#)].
- [82] A. Sabry, *Fourth order spectral functions for the electron propagator*, *Nucl. Phys.* **33** (1962) 401–430.
- [83] E. Remiddi and L. Tancredi, *Differential equations and dispersion relations for Feynman amplitudes. The two-loop massive sunrise and the kite integral*, *Nucl. Phys. B* **907** (2016) 400–444, [[1602.01481](#)].
- [84] L. Adams, C. Bogner, A. Schweitzer and S. Weinzierl, *The kite integral to all orders in terms of elliptic polylogarithms*, *J. Math. Phys.* **57** (2016) 122302, [[1607.01571](#)].
- [85] C. Duhr, F. Gasparotto, C. Nega, L. Tancredi and S. Weinzierl, *On the electron self-energy to three loops in QED*, [2408.05154](#).
- [86] S. Pögel, X. Wang and S. Weinzierl, *Taming Calabi-Yau Feynman Integrals: The Four-Loop Equal-Mass Banana Integral*, *Phys. Rev. Lett.* **130** (2023) 101601, [[2211.04292](#)].
- [87] J. L. Bourjaily et al., *Functions Beyond Multiple Polylogarithms for Precision Collider Physics*, in *Snowmass 2021*, 3, 2022, [2203.07088](#).
- [88] S. Weinzierl, *Feynman Integrals. A Comprehensive Treatment for Students and Researchers*. UNITEXT for Physics. Springer, 2022, [10.1007/978-3-030-99558-4](#).
- [89] X. Jiang, X. Wang, L. L. Yang and J.-B. Zhao, *ε -factorized differential equations for two-loop non-planar triangle Feynman integrals with elliptic curves*, [2305.13951](#).
- [90] L. Görge, C. Nega, L. Tancredi and F. J. Wagner, *On a procedure to derive ε -factorised differential equations beyond polylogarithms*, *JHEP* **07** (2023) 206, [[2305.14090](#)].
- [91] S. Pögel, X. Wang and S. Weinzierl, *The three-loop equal-mass banana integral in ε -factorised form with meromorphic modular forms*, *JHEP* **09** (2022) 062, [[2207.12893](#)].
- [92] S. Pögel, X. Wang and S. Weinzierl, *Bananas of equal mass: any loop, any order in the dimensional regularisation parameter*, *JHEP* **04** (2023) 117, [[2212.08908](#)].
- [93] H. A. Verrill, *Root lattices and pencils of varieties*, *Journal of Mathematics of Kyoto University* **36** (1996) 423 – 446.
- [94] R. N. Lee, *LiteRed 1.4: a powerful tool for reduction of multiloop integrals*, *J. Phys. Conf. Ser.* **523** (2014) 012059, [[1310.1145](#)].
- [95] R. P. Agarwal and D. O’Regan, *Ordinary and partial differential equations: with special functions, Fourier series, and boundary value problems*. Springer Science & Business Media, 2008.
- [96] M. Bogner, *Algebraic characterization of differential operators of calabi-yau type*, [1304.5434](#).
- [97] C. Duhr, A. Klemm, C. Nega and L. Tancredi, *The ice cone family and iterated integrals for Calabi-Yau varieties*, *JHEP* **02** (2023) 228, [[2212.09550](#)].
- [98] F. Forner, *Differential Equations and Dispersion Relations for Feynman Integrals: An Application to QED Two-Point Functions*, 2024.